



國立臺灣大學電機資訊學院光電工程學研究所

碩士論文

Graduate Institute of Photonics and Optoelectronics  
College of Electrical Engineering and Computer Science

National Taiwan University

Master Thesis

活體倍頻顯微術：

皮膚內在老化於活性表皮與真皮乳突之定量分析  
Quantitative Analysis of Intrinsic Skin Aging in Viable  
Epidermis and Dermal Papillae by *In Vivo* Harmonic  
Generation Microscopy

周信佑

Sin-Yo Chou

指導教授：孫啟光 博士

Advisor: Chi-Kuang Sun, Ph.D.

中華民國102年11月

November 2013



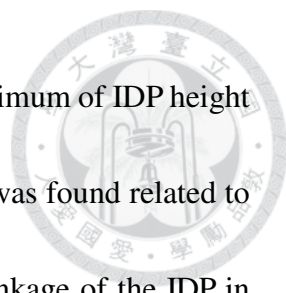
# Abstract



Intrinsic aging of skin is a natural process genetically determined and inalterable.

The aging-related changes increase the susceptibility of skin and reduced the skin barrier function, which increases incidence of inflammatory or infectious skin disorders in the elderly people. To reveal the changes of intrinsic skin aging, a 1230 nm femtosecond Cr:forsterite laser was used as the excitation, and the non-invasive harmonic generation biopsy (HGB) system collecting second-harmonic generation and third-harmonic generation signals was applied to acquire *in vivo* images with high spatial resolution from ventral forearms of 48 Asians with Fitzpatrick skin phototype III or IV. Using the HGB system, the XYZ image stacks of equally-spaced parallel horizontal sections were acquired with step size 2  $\mu\text{m}$  or 5  $\mu\text{m}$  beginning from the stratum corneum into the upper reticular dermis of the skin. Using XYZ image stacks, 14 parameters were defined to inspect morphological changes of viable epidermis and mainly dermal papillae in a three-dimensional point of view.

In the *in vivo* analysis of viable epidermis thickness, viable epidermis thickness excluding rete ridge was not found related to neither age nor gender, but viable epidermis thickness including rete ridge decreased with age. Results together implied that the dermal-epidermal junction flattened in the aged skin. In the *in vivo* analysis of



isolated dermal papilla (IDP), the average, intra-subject SD, and maximum of IDP height and volume all decreased with age. Only the average of IDP height was found related to gender. The results indicated that intrinsic aging resulted in the shrinkage of the IDP in size, and there were only small IDPs remained in the elder skin. In the *in vivo* analysis of dermal papillae within dermal papilla zone (DPZ), both depth of DPZ and 3D interdigitation index decreased with age, but dermal papillae volume ratio within DPZ increased with age. However, number density of dermal papillae, dermal papillae volume per unit area, and average volume per dermal papillae were not found related to age. The results indicated that dermal-epidermal junction became flatter with age, but the dermal papillae within DPZ were not reduced in volume. The independent dermal papillae connected to each other quicker with age, and the whole dermal papillae within DPZ extended in width. Moreover, the analysis of 3D interdigitation index showed the decreasing interface area of dermal-epidermal junction with age, which might related to the fragility of the aged skin due to the weakening of epidermal-dermal adherence.


**Keywords:** harmonic generation microscopy, *in vivo* imaging, intrinsic aging, viable epidermis, dermal papillae

## 摘要



皮膚的內在老化是一個由先天基因所決定且無法改變的自然過程。老化所造成的改變增加了皮膚的敏感性，也減弱了皮膚的防護功能，這樣的情況增加了老年人得到皮膚炎症(inflammation)及皮膚傳染疾病的發生率。為了揭露皮膚的內在老化，我們將一台波長為 1230 奈米的飛秒鎂：鎂橄欖石雷射作為光源，並將包含二倍頻及三倍頻訊號的非侵入式倍頻切片系統運用於取得高解析度的活體人體皮膚影像。我們一共取得了 48 名亞洲受試者的前臂內側皮膚的活體影像，受試者的膚色分類(Fitzpatrick skin phototype)皆為第三或第四類。我們從每位受試者的皮膚取得了間距相同的三維水平切面影像序列，影像的取得由角質層(stratum corneum)一直深入到上層網狀真皮層(reticular dermis)，而影像間距則被設定為 2 微米或 5 微米。利用三維水平切面影像序列，我們定義了 14 個參數，以三維的觀點來檢視活性表皮(viable epidermis)與真皮乳突(dermal papillae)的型態改變。

在活性表皮厚度的活體分析中，我們並未發現不包含網嵴(rete ridge)的活性表皮厚度與年齡或性別相關，而包含網嵴的活性表皮厚度則隨著年齡增加而下降。分析結果暗示著真皮與表皮接合處(dermal-epidermal junction)在老化的皮膚中變得平坦。在孤立真皮乳突(isolated dermal papilla)的活體分析中，孤立真皮乳突高度和體積的平均、自身標準差與最大值皆隨著年齡增加而下降。其中只有孤立真皮乳突高度的平均與性別相關。此分析結果指出，內在老化造成了孤立真皮乳突的體



型縮減，而在老化的皮膚中只剩下較小的孤立真皮乳突。在真皮乳突區域(dermal papilla zone)內的真皮乳突活體分析中，真皮乳突區域之厚度與三維叉合(interdigitation)指標皆隨著年齡增加而下降，而真皮乳突區域內真皮乳突體積比例則隨著年齡增加而上升。不過，真皮乳突數量密度、單位面積所含真皮乳突體積和真皮乳突平均體積則未發現與年齡之相關性。該分析的結果指出真皮與表皮接合處隨著年齡增加而變得平坦，但真皮乳突區域內真皮乳突的體積並未隨著年齡減少。隨著年齡增加，獨立的真皮乳突變得較快與其他乳突相連接，而在真皮乳突區域內整體的真皮乳突變得較寬。此外，三維叉合指標的分析顯示，真皮與表皮接合處的面積隨著老化而減少，這可能與老化皮膚的真皮與表皮黏附力減弱有關，並導致脆弱的老化皮膚。

**關鍵詞：** 倍頻顯微術、活體成像、內在老化、活性表皮、真皮乳突

# Contents



口試委員審定書	
Abstract.....	i
摘要.....	iii
Contents.....	v
Figure Contents.....	vii
Table Contents.....	xii
Chapter 1 Introduction.....	1
1.1 Skin Aging.....	1
1.2 Harmonic Generation Microscopy.....	2
1.3 Comparison between SHGM and SHOCT.....	4
Chapter 2 Materials and Methods.....	6
2.1 Study Population.....	6
2.2 Harmonic Generation Biopsy System.....	6
2.3 Imaging Procedure.....	9
2.4 Analysis Protocols.....	10
2.4.1 Height, Surface Area, and Volume Estimation.....	10
2.4.2 <i>In Vivo</i> Analysis of Viable Epidermis Thickness.....	12
2.4.3 <i>In Vivo</i> Analysis of Isolated Dermal Papilla.....	13
2.4.3.1 Isolated Dermal Papilla.....	13
2.4.3.2 Height of Isolated Dermal Papilla.....	15
2.4.3.3 Volume of Isolated Dermal Papilla.....	16
2.4.4 <i>In Vivo</i> Analysis of Dermal Papillae within Dermal Papilla Zone.....	16
2.4.4.1 Dermal Papilla Zone.....	16
2.4.4.2 Depth of Dermal Papilla Zone.....	19
2.4.4.3 Number Density of Dermal Papillae.....	19
2.4.4.4 Dermal Papillae Volume per Unit Area.....	20
2.4.4.5 Average Volume per Dermal Papilla.....	20
2.4.4.6 Dermal Papillae Volume Ratio within Dermal Papilla Zone.....	21
2.4.4.7 3D Interdigitation Index.....	21
2.5 Statistics Protocol.....	22
Chapter 3 Results.....	24
3.1 <i>In Vivo</i> Image Stacks of Human Skin.....	24
3.2 <i>In Vivo</i> Analysis of Viable Epidermis Thickness.....	24
3.3 <i>In Vivo</i> Analysis of Isolated Dermal Papilla.....	27

3.3.1 Height of Isolated Dermal Papilla .....	27
3.3.2 Volume of Isolated Dermal Papilla.....	30
3.4 <i>In Vivo</i> Analysis of Dermal Papillae within Dermal Papilla Zone.....	32
3.4.1 Depth of Dermal Papilla Zone.....	32
3.4.2 Number Density of Dermal Papillae .....	33
3.4.3 Dermal Papillae Volume per Unit Area .....	34
3.4.4 Average Volume per Dermal Papilla.....	36
3.4.5 Dermal Papillae Volume Ratio within Dermal Papilla Zone.....	37
3.4.6 3D Interdigitation Index .....	39
Chapter 4 Discussion.....	40
4.1 Overall Results of <i>In Vivo</i> Aging Analysis .....	40
4.2 Comparisons of Previous Studies .....	41
4.2.1 Comparison between Results of Depth of Dermal Papilla Zone.....	41
4.2.2 Comparison between Results of 3D Interdigitation Index .....	41
4.2.3 Comparison between Results of Viable Epidermis Thickness .....	42
4.2.4 Comparison between Results of Number Density of Dermal Papillae .	43
4.3 Deduction of Intrinsic Age-Related Changes of Skin .....	46
4.3.1 Deduction of Age-Related Changes of Isolated Dermal Papillae .....	47
4.3.2 Deduction of Age-Related Changes of Dermal Papillae within Dermal Papilla Zone.....	50
4.4 Discussion of Critical Parameters in this Analysis.....	57
Chapter 5 Conclusion .....	59
Reference.....	61



# Figure Contents

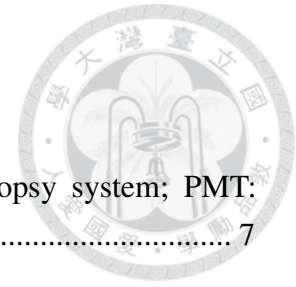


Fig. 1. A schema of the 1230 nm-based harmonic generation biopsy system; PMT: photomultiplier tube; DBS: dichroic beam splitter..... 7

Fig. 2. A Part of a representative XYZ image stack combing SHG and THG signals from a 24-year-old female subject. The image stack recorded different skin layers including stratum corneum (SC), stratum granulosum (SG), stratum spinosum (SS), stratum basale (SB), papillary dermis (PD), and upper reticular dermis (RD). The depths of images were labeled, and the depth of the first frame of the stack that showed the stratum corneum was set as 0  $\mu\text{m}$ . SHG and THG signals were represented by pseudo-colors green and purple. Image dimensions were 240  $\mu\text{m}$   $\times$  240  $\mu\text{m}$ . ..... 8

Fig. 3. A chart showed the rectangular estimation, which approximated an object by a pile of cylinders. The volume and surface area of the object could be estimated by measuring the section areas, their circumferences, and step sizes between sections. .... 11

Fig. 4. Four consecutive frames of an image stack from the ventral forearm of a 24-year-old female subject. The cross-sections of isolated dermal papillae were observed as independent round areas (arrows), and connected with each other in the following frame (arrow heads). Image dimensions were 240  $\mu\text{m}$   $\times$  240  $\mu\text{m}$ . The distances between images were 5  $\mu\text{m}$ . SHG and THG signals were represented by pseudo-colors green and purple. .... 14

Fig. 5. Diagrams of (a) isolated dermal papillae and (b) dermal papillae within dermal papilla zone (DPZ), which were denoted by the green areas. Dermal papilla zone was the region between two dotted lines in (b). ..... 15

Fig. 6. Diagrams showed the required measurements for calculating the parameters defined in the analysis of dermal papillae within DPZ. The total number, the total interface area, the max occupied section area of dermal papillae within DPZ were specified in (a); the depth of DPZ and the total dermal papillae volume within DPZ were specified in (b). ..... 18

Fig. 7. Average thickness of viable epidermis (excluding rete ridge) versus age from the ventral forearms of 47 Asian subjects (skin phototype III & IV). In linear regression analysis, P-value for age = 0.3614 (not statistically significant); P-value for gender = 0.5475 (not statistically significant). In ANOVA, p-value for age group = 0.0107 (statistically significant); p-value for gender = 0.8920 (not statistically significant)..... 26

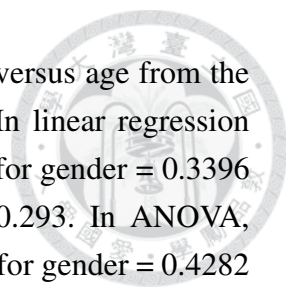


Fig. 8. Average thickness of viable epidermis (including rete ridge) versus age from the ventral forearms of 47 Asian subjects (skin phototype III & IV). In linear regression analysis, P-value for age = 0.0487 (statistically significant); P-value for gender = 0.3396 (not statistically significant). Correlation coefficient R to age = -0.293. In ANOVA, p-value for age group = 0.1592 (not statistically significant); p-value for gender = 0.4282 (not statistically significant). NS: not significant. .... 26

Fig. 9. Average of isolated dermal papilla height versus age from the ventral forearms of 48 Asian subjects (skin phototype III & IV). In linear regression analysis, P-value for age = 0.0003 (statistically significant); P-value for gender = 0.0285 (statistically significant). Correlation coefficient R to age and gender = -0.563. In ANOVA, p-value for age group = 0.0003 (statistically significant); p-value for gender = 0.0975 (not statistically significant). In two lower figures, data of female and male subjects were separately displayed. .... 28

Fig. 10. Intra-subject standard deviation of isolated dermal papilla height versus age from the ventral forearms of 48 Asian subjects (skin phototype III & IV). In linear regression analysis, P-value for age =  $8.315 \times 10^{-5}$  (statistically significant); P-value for gender = 0.4806 (not statistically significant). Correlation coefficient R to age = -0.540. In ANOVA, p-value for age group = 0.0051 (statistically significant); p-value for gender = 0.7703 (not statistically significant). .... 29

Fig. 11. Maximum of isolated dermal papilla height versus age from the ventral forearms of 48 Asian subjects (skin phototype III & IV). In linear regression analysis, P-value for age =  $5.077 \times 10^{-5}$  (statistically significant); P-value for gender = 0.3165 (not statistically significant). Correlation coefficient R to age = -0.551. In ANOVA, p-value for age group = 0.0021 (statistically significant); p-value for gender = 0.5943 (not statistically significant). .... 29

Fig. 12. Average of isolated dermal papilla volume versus age from the ventral forearms of 48 Asian subjects (skin phototype III & IV). In linear regression analysis, P-value for age = 0.0037 (statistically significant); P-value for gender = 0.0930 (not statistically significant). Correlation coefficient R to age = -0.405. In ANOVA, p-value for age group = 0.0128 (statistically significant); p-value for gender = 0.1604 (not statistically significant). .... 31

Fig. 13. Intra-subject SD of isolated dermal papilla volume versus age from the ventral forearms of 48 Asian subjects (skin phototype III & IV). In linear regression analysis, P-value for age = 0.0006 (statistically significant); P-value for gender = 0.5912 (not statistically significant). Correlation coefficient R to age = -0.482. In ANOVA, p-value

for age group = 0.0192 (statistically significant); p-value for gender = 0.7484 (not statistically significant)..... 31

Fig. 14. Maximum of isolated dermal papilla volume versus age from the ventral forearms of 48 Asian subjects (skin phototype III & IV). In linear regression analysis, P-value for age = 0.0005 (statistically significant); P-value for gender = 0.3244 (not statistically significant). Correlation coefficient R to age = -0.482. In ANOVA, p-value for age group = 0.0067 (statistically significant); p-value for gender = 0.4859 (not statistically significant)..... 32

Fig. 15. Depth of dermal papilla zone versus age from the ventral forearms of 48 Asian subjects (skin phototype III & IV). In linear regression analysis, P-value for age = 0.0009 (statistically significant); P-value for gender = 0.0989 (not statistically significant). Correlation coefficient R to age = -0.457. In ANOVA, p-value for age group = 0.0095 (statistically significant); p-value for gender = 0.2017 (not statistically significant)..... 33

Fig. 16. Number density of dermal papillae versus age from the ventral forearms of 48 Asian subjects (skin phototype III & IV). In linear regression analysis, P-value for age = 0.9503 (not statistically significant); P-value for gender = 0.4749 (not statistically significant). In ANOVA, p-value for age group = 0.8096 (not statistically significant); p-value for gender = 0.3678 (not statistically significant). NS: not significant. .... 34

Fig. 17. Dermal papillae volume per unit area versus age from the ventral forearms of 48 Asian subjects (skin phototype III & IV). In linear regression analysis, P-value for age = 0.1471 (not statistically significant); P-value for gender = 0.1287 (not statistically significant). In ANOVA, p-value for age group = 0.4008 (not statistically significant); p-value for gender = 0.1561 (not statistically significant). NS: not significant. .... 35

Fig. 18. Average volume per dermal papilla versus age from the ventral forearms of 48 Asian subjects (skin phototype III & IV). In linear regression analysis, P-value for age = 0.5962 (not statistically significant); P-value for gender = 0.1276 (not statistically significant). In ANOVA, p-value for age group = 0.3120 (not statistically significant); p-value for gender = 0.0920 (not statistically significant). NS: not significant. .... 37

Fig. 19. Dermal papillae volume ratio within dermal papilla zone versus age from the ventral forearms of 48 Asian subjects (skin phototype III & IV). In linear regression analysis, P-value for age = 0.0143 (statistically significant); P-value for gender = 0.3796 (not statistically significant). Correlation coefficient R to age = 0.352. In ANOVA, p-value for age group = 0.0423 (statistically significant); p-value for gender = 0.2307 (not statistically significant)..... 38

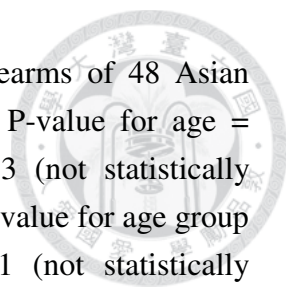


Fig. 20. 3D interdigitation index versus age from the ventral forearms of 48 Asian subjects (skin phototype III & IV). In linear regression analysis, P-value for age =  $2.035 \times 10^{-5}$  (statistically significant); P-value for gender = 0.6453 (not statistically significant). Correlation coefficient R to age = -0.578. In ANOVA, p-value for age group = 0.0013 (statistically significant); p-value for gender = 0.9041 (not statistically significant)..... 39

Fig. 21. Four sets of representative images from the ventral forearms of (a) 27-, (b) 24-, (c) 74-, and (d) 69-year-old subjects. The depths of images were labeled, and the depths of the first frames that showed the stratum corneum in respective stacks were set as 0  $\mu\text{m}$ . In (a) young and (c) elder skin, the cross-sections of isolated dermal papillae seemed to be larger and rounder; however, in other (b) young and (d) elder skin, the cross-sections of isolated dermal papillae appeared to be smaller and fragmentary. This difference between subjects did affect the number density of dermal papillae but was not related to age..... 46

Fig. 22. Coefficient of variance of isolated dermal papilla height (left) versus age from the ventral forearms of 48 Asian subjects (skin phototype III & IV). In linear regression analysis, P-value for age = 0.0144 (statistically significant); P-value for gender = 0.3845 (not statistically significant). Correlation coefficient R to age = -0.352. Coefficient of variance of isolated dermal papilla volume (right) versus age from the ventral forearms of 48 Asian subjects (skin phototype III & IV). In linear regression analysis, P-value for age = 0.0376 (statistically significant); P-value for gender = 0.1055 (not statistically significant). Correlation coefficient R to age = -0.295..... 48

Fig. 23. Average section area of isolated dermal papilla versus age from the ventral forearms of 48 Asian subjects (skin phototype III & IV). In linear regression analysis, P-value for age = 0.6223 (not statistically significant); P-value for gender = 0.1576 (not statistically significant)..... 49

Fig. 24. Diagrams showed how isolated dermal papillae changed with aging. The isolated dermal papillae were shorter and smaller in the elder skin (b), and the sizes became similar. However, the isolated dermal papillae did not extend their widths in the elder skin. .... 50

Fig. 25. Diagrams that showed how dermal papillae within dermal papilla zone changed with aging. In the elder skin, with the thinner dermal papilla zone, the dermal papillae within dermal papilla zone became shorter but extended in width and occupied more proportion of the volume of dermal papilla zone. .... 54

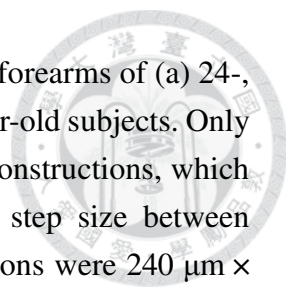


Fig. 26. 3D reconstructions of 9 XYZ image stacks from the ventral forearms of (a) 24-, (b) 27-, (c) 28-, (d) 47-, (e) 47-, (f) 57-, (g) 62-, (h) 69-, and (i) 74-year-old subjects. Only SHG signals within the dermal papilla zone were used in the 3D reconstructions, which revealed the structure of dermal papillae. In (d), (e), and (g), the step size between images was 2  $\mu\text{m}$ , and the X-Y-Z dimensions of the 3D reconstructions were 240  $\mu\text{m}$   $\times$  240  $\mu\text{m}$   $\times$  84  $\mu\text{m}$ . In the others, the step size was 5  $\mu\text{m}$ , and the X-Y-Z dimensions were 240  $\mu\text{m}$   $\times$  240  $\mu\text{m}$   $\times$  85  $\mu\text{m}$ . The coordinate axes were added beside the reconstructions, and z-axes pointed to the deeper dermis. The 3D reconstructions were built by ImageJ 3D Viewer..... 55

# Table Contents



Table 1. Summary of parameter definitions and notations in the <i>in vivo</i> analysis of dermal papillae within dermal papilla zone.....	18
Table 2. The summery of changes with increasing age of parameters in the analysis of dermal papillae within dermal papilla zone.....	50
Table 3. Depth of DPZ, DP volume per unit area, DP volume ratio within DPZ, and 3D interdigitation index for each image stack in Fig. 26 .....	55

# Chapter 1 Introduction



## 1.1 Skin Aging

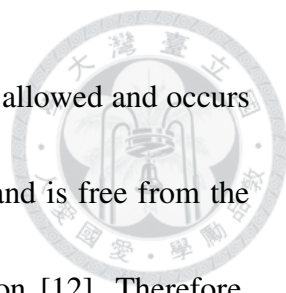
Aging is a process of structural integrity loss and physiological changes caused by both intrinsic and extrinsic factors. Intrinsic aging of skin is a natural process genetically determined and inalterable. However, extrinsic aging of skin is affected by relatively controllable factors, and the effects of sunlight exposure are estimated to account for up to 90% of the visible skin aging [1]. Morphologic changes related to intrinsic aging in older skin are relatively subtle and consist of primary laxity, fine wrinkling, and a variety of benign neoplasms [2]. The aging-related changes include fewer basal keratinocytes, decreased vascularity, fewer sweat glands, and flattened dermal-epidermal junction [2]. These changes increase the susceptibility of skin and reduced the skin barrier function, which increases incidence of inflammatory or infectious skin disorders in the elderly people [2]. In fact, most people in America over 65 have at least one skin disorder, and many have two or more [3]. As the proportion of people who are elderly is increasing, the issue of skin aging is becoming more and more important.

## 1.2 Harmonic Generation Microscopy



Although skin biopsy is the most generally used technique to evaluate morphologic changes in dermatological study, its invasive nature makes it not a suitable method to investigate skin aging. The harmonic generation microscopy could be a more adaptive technique for revealing the changes of intrinsic skin aging due to its capability of non-invasive *in vivo* imaging with a high spatial resolution. The harmonic generations are nonlinear optical processes, in which virtual-level transitions are involved. Through the induction of electric polarization, the second-harmonic generation (SHG) process is the generation of light with the frequency that is twice the frequency of the excitation (fundamental) light, and the third-harmonic generation (THG) is the generation of light with the frequency that is triple the frequency of the excitation light [4]. Due to only the virtual-level transition involved, the SHG and THG processes leave no energy and cause no photodamage [5, 6]. Moreover, the intensities of the SHG and THG generated were proportional to square and cubic of the excitation light intensity respectively and both signals are generated only in close proximity to the focal point. Therefore, the confined excitation volume can provide high resolution of three-dimensional image [7, 8]. In theory, SHG only occurs from optically non-centrosymmetric media, such as collagen fibers and muscle fibers [9-11]. Therefore, SHG microscopy is ideal for investigate



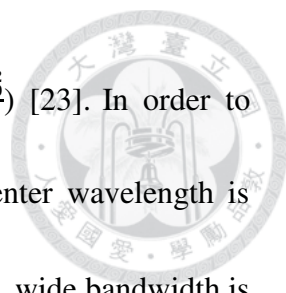


collagenous structures in the dermis. THG is a process that is dipole allowed and occurs in all materials. Moreover, THG occurs at interfaces of any media and is free from the constraint of a phase-matching condition and wavelength restriction [12]. Therefore, THG can provide the information of bio-tissues and cellular morphology. In the previous studies, THG was reported to arise from the cell membrane [13] and the cytoplasmic organelles [8], and to be enhanced by melanin [14], oxy-hemoglobin [15], and elastin [16] through resonance enhancement [17]. In our previous studies, a femtosecond Cr:forsterite laser at 1230 nm was used as the excitation source of the harmonic generation microscopy combining both SHG and THG, which was used for the non-invasive *in vivo* optical virtual biopsy on human skin without damage. This harmonic generation biopsy could clearly reveal *in vivo* skin structure from the outermost stratum corneum to the upper dermis [16, 18]. In this study, the harmonic generation biopsy system was applied to investigate structural changes of epidermis and dermis related to intrinsic aging.

### 1.3 Comparison between SHGM and SHOCT



Second harmonic optical coherence tomography (SHOCT) is an extension of the OCT that can provide additional information by collecting SHG signals for imaging [19-22]. Compared with second harmonic generation microscopy (SHGM), SHOCT also collects SHG signals from non-centrosymmetric media and possesses the advantages of harmonic generation, such as no photodamage and confined excitation volume. For the system setup, because SHOCT needs to split the source light first to generate a reference second-harmonic light by a nonlinear crystal and then recombine it with the second-harmonic signal generated from sample, SHOCT requires a more complicated system setup. For the spatial resolutions, SHOCT could achieve axial resolution of several micrometers determined by the coherence length and lateral resolution of few micrometers determined by the spot size, such as 4.2  $\mu\text{m}$  and 1.9  $\mu\text{m}$  reported by Jiang *et al.* [22]. However, using high NA objective, SHGM could achieve axial and lateral resolution of  $\sim 1 \mu\text{m}$  and sub-micrometer [14, 18]. To improve the lateral resolution of SHOCT, adopting a higher NA objective could narrow the spot size but results in a smaller depth of focus [23]. To improve the axial resolution of SHOCT, the coherence length should be reduced, and the coherence length  $l_c$  was proportional to square of the



center wavelength  $\lambda_0$  and the inverse of bandwidth  $\Delta\lambda$  ( $l_c = \frac{2 \ln 2 \lambda_0^2}{\pi \Delta\lambda}$ ) [23]. In order to prevent large scattering and absorption of the human skin, the center wavelength is preferred in some ranges and could not be too small [23]. Therefore, wide bandwidth is needed to acquire higher resolution. For example, to achieve axial resolution of  $\sim 1 \mu\text{m}$ , bandwidth should be over 70 nm at center wavelength of 400 nm [24]. For the penetration depth, OCT was generally reported to achieve penetration of few millimeters [23]. For SHOCT, the penetration depth was reported to be 280-350  $\mu\text{m}$  in hydrated type I collagen [19] and  $\sim 700 \mu\text{m}$  in fish scales. For SHGM, the penetration depth was reported to be  $\sim 1.5 \text{ mm}$  through zebra fish embryo [25],  $\sim 700 \mu\text{m}$  inside the mouse eye [26], and above 300  $\mu\text{m}$  in the human skin [14, 18]. Therefore, SHOCT and SHGM seem to provide similar depth of penetration in bio-tissues.

## Chapter 2 Materials and Methods



### 2.1 Study Population

48 Asian subjects with 7 females and 8 males aged 19-29 years, 13 females and 6 males aged 30-59 years, and 8 females and 6 males aged 60-79 years, of Fitzpatrick skin phototype III or IV participated. One male subject was not included in the analysis of viable epidermis thickness because his images of viable epidermis were not fully obtained. Subjects with diabetes or skin diseases were excluded. This study was conducted according to the Declaration of Helsinki Principles, and the protocol was approved by the Institutional Review Board of National Taiwan University Hospital. Informed consent was obtained from each subject prior to study entry.

### 2.2 Harmonic Generation Biopsy System

A 1230 nm femtosecond Cr:forsterite laser was used as the excitation to reduce the attenuation from both scattering and absorption of the human skin and to increase the imaging penetrability [27-29]. As described in the previous study [14], the harmonic generation biopsy (HGB) system was adapted from a commercial confocal scanning system (FV300, Olympus, Tokyo, Japan) combined with an inverted microscope (IX71,

Olympus, Tokyo, Japan). A 60X water-immersion objective with NA 1.2 was used in this study, and second- and third-harmonic generation signals were backward-collected by two photomultiplier tubes (Fig. 1). Using this system, subjects only need to put their forearms on the sample stage with ventral side downward, and the imaging depth in the skin could be control by the z-motor with high resolution ( $\sim 0.1 \mu\text{m}$ ). A submicron lateral resolution and  $\sim 1 \mu\text{m}$  axial resolution were achieved. The penetrability  $> 300\mu\text{m}$  could be reached [14, 18].

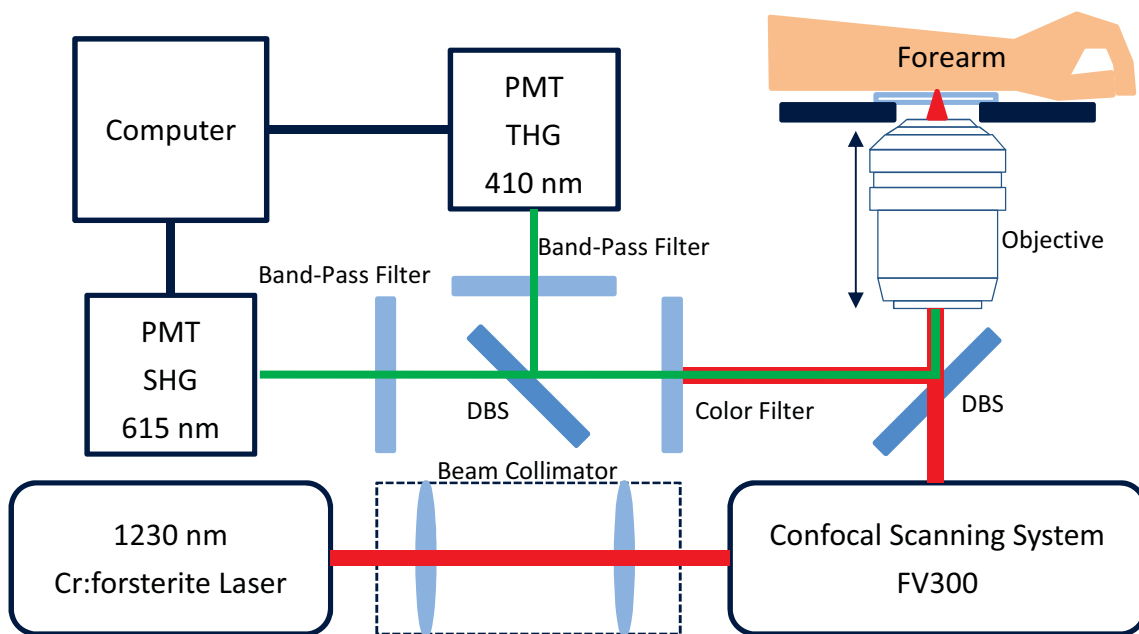


Fig. 1. A schema of the 1230 nm-based harmonic generation biopsy system; PMT: photomultiplier tube; DBS: dichroic beam splitter.

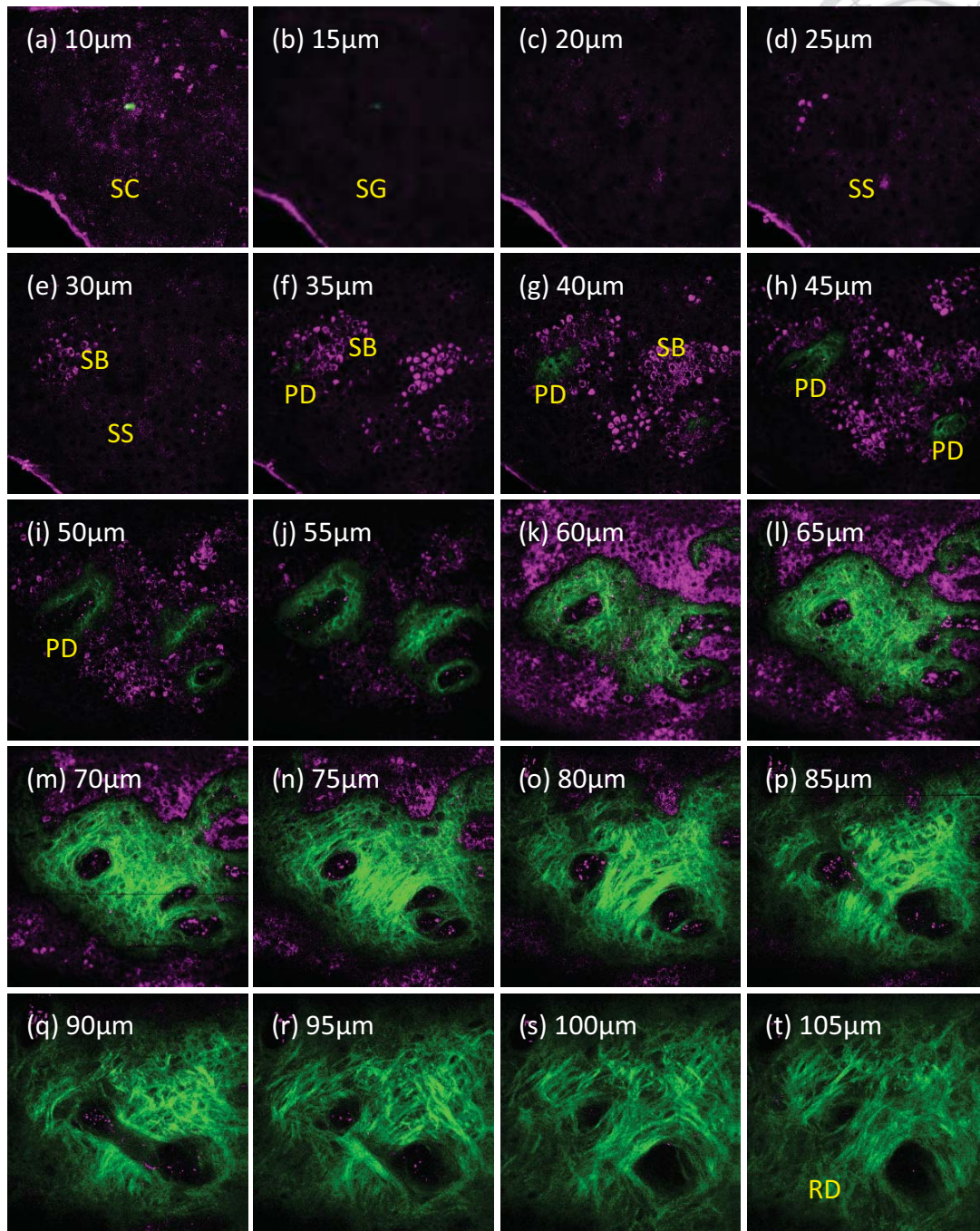
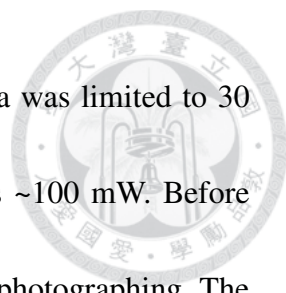


Fig. 2. A Part of a representative XYZ image stack combining SHG and THG signals from a 24-year-old female subject. The image stack recorded different skin layers including stratum corneum (SC), stratum granulosum (SG), stratum spinosum (SS), stratum basale (SB), papillary dermis (PD), and upper reticular dermis (RD). The depths of images were labeled, and the depth of the first frame of the stack that showed the stratum corneum was set as 0  $\mu\text{m}$ . SHG and THG signals were represented by pseudo-colors green and purple. Image dimensions were 240  $\mu\text{m} \times 240 \mu\text{m}$ .

## 2.3 Imaging Procedure



Observations were performed at the left ventral forearms about 15 cm proximal of the subjects' wrists. Using the XYZ mode of the *in vivo* HGB system, the objective could move in the z direction with a specified step size, and image stacks of equally-spaced parallel horizontal sections were acquired with step sizes 2  $\mu\text{m}$  or 5  $\mu\text{m}$ . The XYZ image stacks of skin were obtained beginning from the stratum corneum, through the stratum granulosum, stratum spinosum, stratum basale, papillary dermis, and to the upper reticular dermis (Fig. 2). During the imaging process, the voltages of two photomultiplier tubes were adjusted continuously to keep SHG and THG signals visually bright enough but not saturated. Each image frame was with  $512 \times 512$  pixels, and the actual spatial dimensions were  $240 \mu\text{m} \times 240 \mu\text{m}$  or  $200 \mu\text{m} \times 200 \mu\text{m}$ . In this study, the image stacks were excluded if the section images in them were not horizontal to the skin, which obviously changed with depth non-uniformly in different corners. Image stacks were also excluded if they had more than two successive blurred frames. Total 200 XYZ image stacks including 14 stacks with step size 2  $\mu\text{m}$  and 186 stacks with step size 5  $\mu\text{m}$  were analyzed. The maximum, minimum, and average numbers of the image stacks obtained from one subject were 2, 10, and 4.167. The imaging trials of 13 subjects were carried out by me.



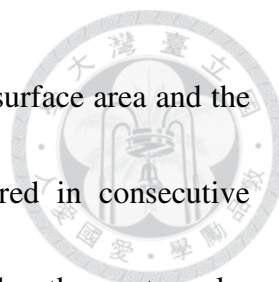
For each subject, the total laser exposure time in the same area was limited to 30 minutes, and the average power measured right after objective was ~100 mW. Before and after the HGB, the test sites of all volunteers were recorded by photographing. The volunteers were informed to feel free to contact us if they felt any discomfort during or after HGB. There were no cutaneous side effects observed such as erythema, pigment alteration, ulceration or blister formation. The procedure was comfortable and caused no itch or pain according to volunteers' opinions.

## **2.4 Analysis Protocols**

### **2.4.1 Height, Surface Area, and Volume Estimation**

To understand the morphological features of viable epidermis and the dermal papillae (DP), the analysis was performed on the image stacks of equally-spaced parallel horizontal sections. From these image stacks, the height, the surface area, and the volume were measured for analysis. Because the objective was water-immersed, of which the refraction index was close to that of skin, the refraction of light was neglected. Therefore, the distance between section images in the skin was approximated by the step size of the objective movement. The height was calculated by counting the number





of the consecutive frames and multiplying by the step size. For the surface area and the volume, the section areas and their circumferences were measured in consecutive frames, and the volume and the surface area were estimated by the rectangular estimation, which approximated the real object by a pile of irregular cylinders (Fig. 3). For the volume estimation, calculation was done by summing up the section areas multiplied by the step size. With the same principle, the surface area was calculated by adding all the products of the circumference and the step size, the area differences between the pairs of section areas in two successive frames, and the top section area.

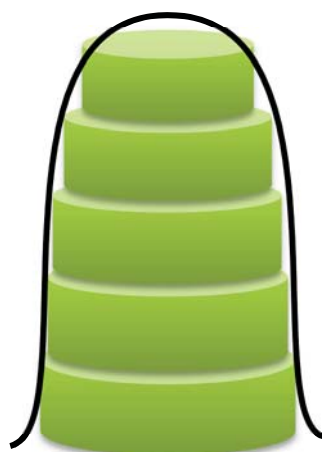
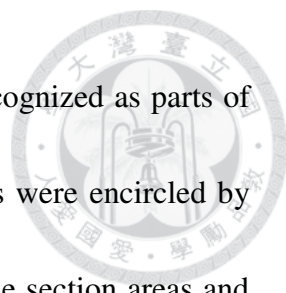


Fig. 3. A chart showed the rectangular estimation, which approximated an object by a pile of cylinders. The volume and surface area of the object could be estimated by measuring the section areas, their circumferences, and step sizes between sections.

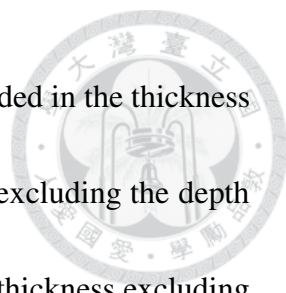
For the estimations of the volume and the surface area, which was more proper to be called as the interface area, of dermal papillae, it should be noted that the tiny spaces between collagen fibers and the capillaries inside the dermal papillae, which were



observed as dark holes surrounded by the SHG signals, were all recognized as parts of dermal papillae. In other words, if these tiny spaces and dark holes were encircled by the SHG signals, they would be included in the measurements of the section areas and their circumferences. Using the estimated height, the interface area, and the volume, several parameters were defined: the thickness of viable epidermis, the height of isolated dermal papilla, the volume of isolated dermal papilla, the depth of dermal papilla zone, the number density of dermal papilla, the dermal papillae volume per unit area, the average volume per dermal papilla, the dermal papillae volume ratio within dermal papilla zone, and the 3D interdigitation index.

#### **2.4.2 *In Vivo* Analysis of Viable Epidermis Thickness**

Beneath stratum corneum lay the viable epidermis, which included stratum granulosum, stratum spinosum, and stratum basale, where keratinocytes with nuclei could be observed. Such as in Fig. 2(a), no cells with nuclei were observed in the stratum corneum, and then cells with nuclei first appeared in the stratum granulosum in Fig. 2(b), where was defined as the topmost layer of the viable epidermis. The thickness of viable epidermis was measured from stratum granulosum to stratum basale. However, the interface between epidermis and dermis was an undulated surface, and whether rete ridge,



which were the protrusions of epidermis into dermis, should be included in the thickness measurement was an issue. Therefore, measurements including and excluding the depth of rete ridge were both performed. Therefore, such as in Fig. 2, the thickness excluding rete ridge was the step size multiplied by the count of frames from (b) to (e), and the thickness including rete ridge was the step size multiplied by the count of frames from (b) to (q). Both thicknesses were measured for every image stack, and average and standard deviation (SD) of a subject were calculated based on the respective thicknesses of all his or her image stacks.

### **2.4.3 *In Vivo* Analysis of Isolated Dermal Papilla**

#### **2.4.3.1 Isolated Dermal Papilla**

The dermal papillae were the individual protrusions of dermis to epidermis, and as the observation got deeper into the skin, they joined together to form the papillary dermis. In our XYZ image stacks, after the basal cells appeared in the upper layer, the cross-sections of the upper-part dermal papillae were observed as independent round areas (Fig. 4). As it got deeper, these independent round areas gradually became larger, then connected with others, and finally joined together. These independent protrusions of upper-part dermal papillae were called isolated dermal papillae and were focused in

this part of analysis (Fig. 5(a)). In the XYZ image stacks, these independent round areas were identified as the sections of the isolated dermal papillae before they connected with others. If a cross-section of an isolated dermal papilla was cut by the border of image, it would be excluded in the measurements of height and volume. These independent cross-section areas of isolated dermal papillae in the frame where they first appeared were recorded and assigned numbers respectively, and the cross-section areas from the same isolated dermal papillae in the following frames, which were identified by their locations, were assigned the same numbers and recorded. The measurement and recording ended when the cross-sections connected to each other. The data of an isolated dermal papilla with the same assigned number were used to calculate its height and volume.

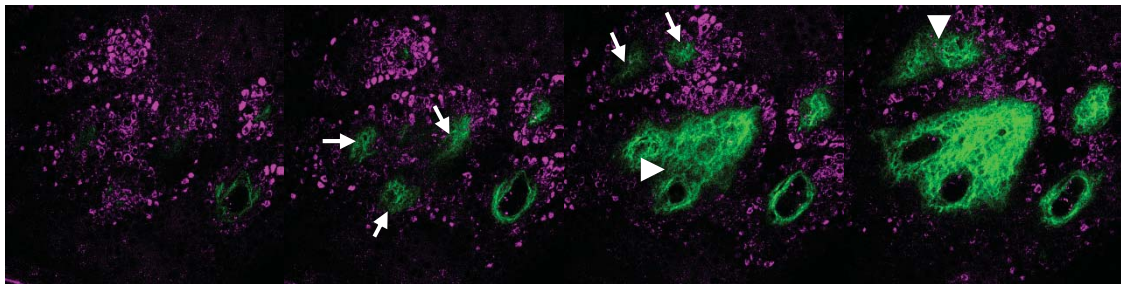


Fig. 4. Four consecutive frames of an image stack from the ventral forearm of a 24-year-old female subject. The cross-sections of isolated dermal papillae were observed as independent round areas (arrows), and connected with each other in the following frame (arrow heads). Image dimensions were  $240\ \mu\text{m} \times 240\ \mu\text{m}$ . The distances between images were  $5\ \mu\text{m}$ . SHG and THG signals were represented by pseudo-colors green and purple.

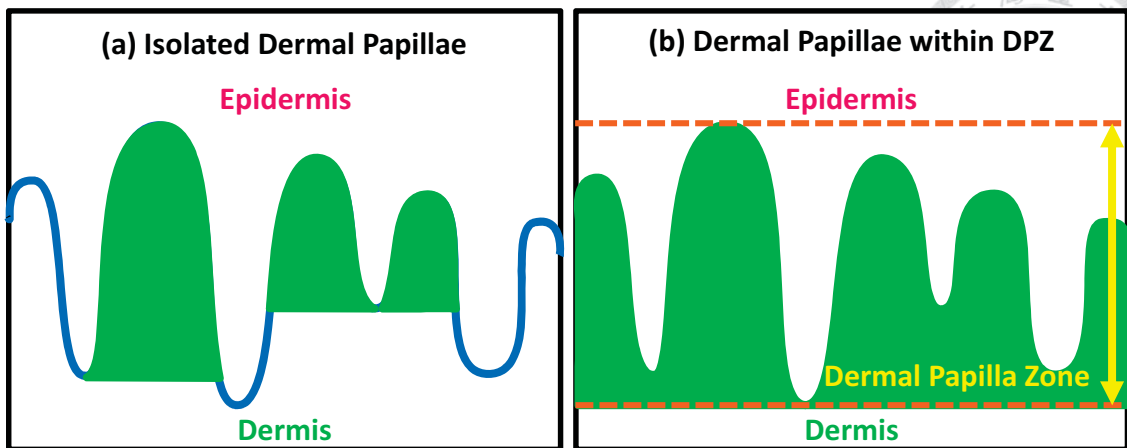


Fig. 5. Diagrams of (a) isolated dermal papillae and (b) dermal papillae within dermal papilla zone (DPZ), which were denoted by the green areas. Dermal papilla zone was the region between two dotted lines in (b).

#### 2.4.3.2 Height of Isolated Dermal Papilla

The respective heights of isolated dermal papillae observed in all image stacks from a subject were measured. For each subject, at least 5 isolated dermal papillae were included for height measurement, and the average, the intra-subject standard deviation, and the maximum (top 20%) of isolated dermal papilla height were calculated based on the results of all his or her isolated dermal papillae. It should be clarified that the average, the intra-subject SD, and the maximum were not acquired for each stack and then averaged for a subject, but directly calculated from the respective heights of all his or her isolated dermal papillae.




### **2.4.3.3 Volume of Isolated Dermal Papilla**

The volume of each isolated dermal papilla in each image stack from a subject was calculated by the rectangle estimation. For each subject, the average, the intra-subject standard deviation, and the maximum of isolated dermal papilla volume were computed as well based on all his or her isolated dermal papillae, and the number of isolated dermal papillae should be no less than 5. It should be also clarified that that the average, the intra-subject SD, and the maximum were directly calculated from the respective volumes of all his or her isolated dermal papillae.

### **2.4.4 *In Vivo* Analysis of Dermal Papillae within Dermal Papilla Zone**

#### **2.4.4.1 Dermal Papilla Zone**

In the human skin, epidermis and dermis interdigitated at the interface, dermal-epidermal junction, and the dermal papilla zone was defined as the layer where epidermis and dermis both existed. Therefore, in the XYZ image stacks, the dermal papilla zone started when the dermis appeared in the shallower layer, and ended when the epidermis disappeared (Fig. 5(b)). The features of dermal papillae within the dermal papilla zone were focused in the following analysis. The total occupied section area and its circumference of dermal papillae were recorded for each frame within dermal papilla



zone in order to calculate following parameters. If part of the circumference overlapped border lines of the frame, the length of that part was excluded in the measurement. As it got deeper, dermal papillae would occupy more area in the frame. However, for most of the XYZ stacks, the occupied section area of dermal papillae did not occupy whole frame area in the deepest frame within the dermal papilla zone, and sweat glands appeared occasionally, which were excluded in the measurement. Sweat glands were observed as large dark holes surrounded by THG signals of cells in dermis. In addition, the max occupied section area was generally found in the last frame within dermal papilla zone, but slight decreases of the last frames in some stacks could be found due to truly decreased occupied area, appearance of sweat glands, or errors of manual selections. Therefore, the bottom area of the dermal papilla zone was defined as the max occupied section area of the dermal papillae instead of the whole frame area.

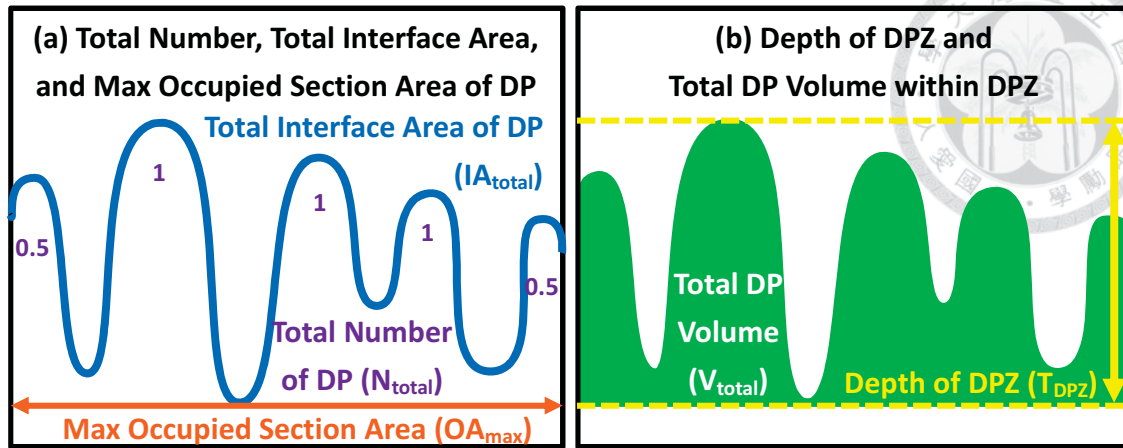


Fig. 6. Diagrams showed the required measurements for calculating the parameters defined in the analysis of dermal papillae within DPZ. The total number, the total interface area, the max occupied section area of dermal papillae within DPZ were specified in (a); the depth of DPZ and the total dermal papillae volume within DPZ were specified in (b).

**Table 1. Summary of parameter definitions and notations in the *in vivo* analysis of dermal papillae within dermal papilla zone**

Parameter	Definition	Notation
Depth of DPZ ( $T_{DPZ}$ )	Depth of DPZ	$T_{DPZ}$
Number Density of DP ( $D_N$ )	$\frac{\text{Total DP Number}}{\text{Max DP Occupied Section Area}}$	$\frac{N_{total}}{OA_{max}}$
DP Volume per Unit Area ( $D_V$ )	$\frac{\text{Total DP Volume}}{\text{Max DP Occupied Section Area}}$	$\frac{V_{total}}{OA_{max}}$
Average Volume per DP ( $V_{DP}$ )	$\frac{\text{Total DP Volume}}{\text{Total DP Number}}$	$\frac{V_{total}}{N_{total}}$
DP Volume Ratio within DPZ ( $R_V$ )	$\frac{\text{Total DP Volume}}{\text{Max DP Occupied Section Area} \times \text{Depth of DPZ}}$	$\frac{V_{total}}{OA_{max} \times T_{DPZ}}$
3D Interdigitation Index ( $I_{3D}$ )	$\frac{\text{Total DP Interface Area}}{\text{Max DP Occupied Section Area}}$	$\frac{IA_{total}}{OA_{max}}$





#### **2.4.4.2 Depth of Dermal Papilla Zone**

The depth of dermal papilla zone ( $T_{DPZ}$ ; Fig. 6(b)) was measured by counting the frames from the first observation of dermal papillae to the last observation of basal cells and multiplying by the step size for each image stack. For a subject, the respective depth of dermal papilla zone for each of his or her stack was obtained. Based on these depths, the depth of a subject was acquired from the average of stacks, and the intra-subject SD was calculated. The change of the depth of dermal papilla zone could indicate whether the dermal-epidermal junction flattened or sharpened.

#### **2.4.4.3 Number Density of Dermal Papillae**

To understand the distribution of dermal papillae, the number of dermal papillae was acquired by simply counting the number of isolated dermal papillae. In each XYZ image stack, the total number of dermal papillae (Fig. 6(a)) was counted, among which an incomplete one was counted as 0.5, and the max occupied section area of dermal papillae within dermal papilla zone was measured (Fig. 6(a)). The number density of dermal papillae ( $D_N$ ) for a subject was calculated by the sum of the total number of dermal papillae ( $N_{total}$ ) obtained from all his or her stacks divided by the sum of the max occupied section area ( $OA_{max}$ ). For a subject, the respective number density of every his



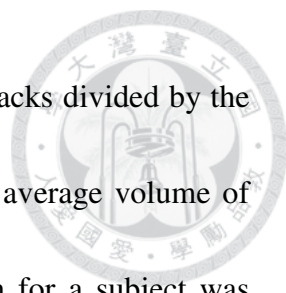
or her stack was also calculated, and the intra-subject standard deviation was obtained between these number densities.

#### **2.4.4.4 Dermal Papillae Volume per Unit Area**

The dermal papillae volume per unit area ( $D_V$ ) of a subject, which revealed how much volume of dermal papillae spread on the skin, was calculated by the sum of the total dermal papillae volume ( $V_{\text{total}}$ ; Fig. 6(b)) from all his or her image stacks divided by the sum of the max occupied section area of dermal papillae within dermal papilla zone ( $OA_{\text{max}}$ ; Fig. 6(a)). The volume per unit area of each stack was calculated, and the intra-subject standard deviation for a subject was obtained between the respective results of his or her stacks.

#### **2.4.4.5 Average Volume per Dermal Papilla**

In the analysis of isolated dermal papilla, only the upper-part dermal papillae that did not connect to each other were analyzed. In this part of analysis, it was defined that the bottom of each dermal papilla was as deep as the bottom of dermal papilla zone, so the connected-part of dermal papillae within dermal papilla zone was included for acquiring the volume of one dermal papilla. Average volume per dermal papilla ( $V_{\text{DP}}$ ) of a subject was estimated by the sum of the total dermal papillae volume within dermal



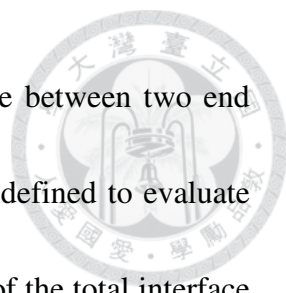
papilla zone ( $V_{total}$ ; Fig. 6(b)) measured from all his or her image stacks divided by the sum of the total number of dermal papillae ( $N_{total}$ ; Fig. 6(a)). The average volume of each stack was calculated, and the intra-subject standard deviation for a subject was obtained between the respective average volumes of his or her stacks.

#### **2.4.4.6 Dermal Papillae Volume Ratio within Dermal Papilla Zone**

To indicate how much volume of dermal papilla zone was occupied by dermal papillae, the dermal papillae volume ratio within dermal papilla zone ( $R_V$ ) of a subject was calculated from the sum of the total dermal papillae volume within dermal papilla zone ( $V_{total}$ ; Fig. 6(b)) in all his or her stacks divided by the sum of the volume of dermal papilla zone, which was the max occupied section area of dermal papillae ( $OA_{max}$ ; Fig. 6(a)) multiplied by the depth of dermal papilla zone ( $T_{DPZ}$ ; Fig. 6(b)). The ratio of each stack was calculated, and the intra-subject standard deviation of a subject was obtained between the respective ratios of his or her stacks.

#### **2.4.4.7 3D Interdigitation Index**

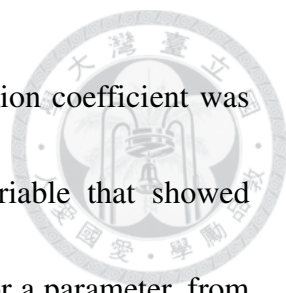
Timár *et al.* [30] introduced the idea of the interdigitation index to measure the undulation of the dermal-epidermal junction. Vertical section of the skin was used, and the interdigitation index was calculated by the length of the curved line along the



dermal-epidermal junction divided by the length of the straight line between two end points. By expanding their idea, 3D interdigitation index ( $I_{3D}$ ) was defined to evaluate the three-dimensional undulation, which was calculated by the sum of the total interface area of dermal papillae ( $IA_{total}$ ; Fig. 6(a)) obtained from all his or her stacks divided by the sum of the max occupied section area of dermal papillae within the dermal papilla zone ( $OA_{max}$ ; Fig. 6(b)) for a subject. The index of each stack was calculated, and the intra-subject standard deviation of a subject was obtained between the respective indexes of his or her stacks.

## 2.5 Statistics Protocol

Statistical analysis was performed with IBM SPSS Statistics ver. 20. A set of parameters and their intra-subject standard deviations was acquired for each subject by the foregoing methods. To investigate age-related changes, the multiple linear regression model with age and gender as variables was used for statistical analysis, and P-values (denoted as P) were acquired for both variables. P-value < 0.05 was considered to be statistically significant. If age and gender both showed statistical significances, correlation coefficient (denoted as R) was acquired from the multiple linear regression



model. If only one variable showed statistical significance, correlation coefficient was acquired from simple linear regression model with only one variable that showed significance. If age and gender showed no statistical significances for a parameter, from all the subjects, the average, the inter-subject standard deviation, and the coefficient of variance (CV), which was the average divided by the standard deviation, were calculated to observe the dispersion of the parameter. To explore the differences among age groups, data were sort by age into groups of 19-29 years, 30-59 years, and 60-79 years. The analysis of variance (ANOVA) was performed with two factors, age group and gender, and statistical significances of both factors (denoted as p) were acquired. If ANOVA showed significance for either factor, post hoc analysis was performed by LSD method to inspect difference of which two groups was significance. If gender showed statistical significance in the multiple linear regression analysis or ANOVA, three age groups were further divided by gender into six groups. The average and standard deviation for each group were calculated and displayed as the average  $\pm$  SD.

## Chapter 3 Results

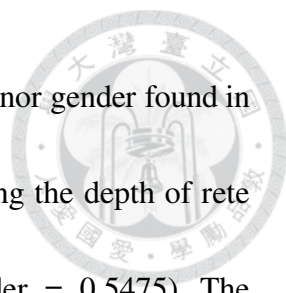


### 3.1 *In Vivo* Image Stacks of Human Skin

Using the harmonic generation biopsy system, a series of human skin images were acquired *in vivo* starting from the stratum corneum to the upper reticular dermis. In the image (a) to the image (e) of Fig. 2, all the layers of epidermis were clearly displayed by the third harmonic generation signals. In the image (f), the second harmonic generation signals showed the appearance of the papillary dermis distinctly. In the following images, the epidermis seemed to diminish and the dermis increased their proportions of image areas. Because the epidermis and dermis were showed by the THG and SHG signals respectively, the interface of epidermis and dermis was clearly displayed. Therefore, the structure of dermal papillae could be distinguished from the epidermis by the SHG signals with fine resolution and surrounding THG signals.

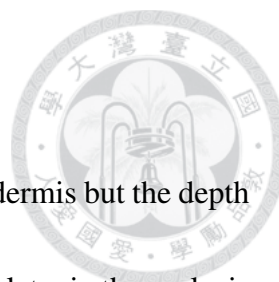
### 3.2 *In Vivo* Analysis of Viable Epidermis Thickness

Although statistical significance of age group was found in ANOVA of the thickness of viable epidermis excluding the depth of rete ridge (Fig. 7;  $p$  for age group =



0.0107 and  $p$  for gender = 0.8920), there was no significance of age nor gender found in the regression analysis of the thickness of viable epidermis excluding the depth of rete ridge (Fig. 7;  $P_{\text{excludeRR}}$  for age = 0.3614 and  $P_{\text{excludeRR}}$  for gender = 0.5475). The thicknesses excluding rete ridge for age groups 19-29, 30-59, and 60-79 years were  $22.76 \pm 2.73 \mu\text{m}$ ,  $27.50 \pm 4.19 \mu\text{m}$ , and  $24.76 \pm 5.14 \mu\text{m}$ . No trend of decrease or increase with age could be observed in Fig. 7. Therefore, the thickness of viable epidermis excluding the depth of rete ridge did not increase or decrease with age. The average and inter-subject standard deviation of the thickness excluding rete ridge from all the subjects was  $25.23 \mu\text{m}$  and  $4.49 \mu\text{m}$ , and the coefficient of variance was 0.1781.

Statistical significance was not found in ANOVA of viable epidermis thickness including the depth of rete ridge (Fig. 8;  $p$  for age group = 0.1592 and  $p$  for gender = 0.4282). However, the result showed significance of age in the regression analysis of viable epidermis thickness including the depth of rete ridge (Fig. 8;  $P_{\text{includeRR}}$  for age = 0.0487 and  $P_{\text{includeRR}}$  for gender = 0.3396). A small and negative correlation was found between age and the thickness of viable epidermis including the depth of rete ridge ( $R = -0.293$ ). The thicknesses including rete ridge for age groups 19-29, 30-59, and 60-79 years were  $91.91 \pm 17.56 \mu\text{m}$ ,  $83.40 \pm 15.97 \mu\text{m}$ , and  $79.10 \pm 17.71 \mu\text{m}$ . The thicknesses including rete ridge seemed to decrease with age, but differences between subjects were



larger than the age-related decreases.

Both results together implied that not the thickness of viable epidermis but the depth of rete ridge decreased with age. This implication would be confirmed later in the analysis of the depth of dermal papilla zone, which was the same as the depth of rete ridge.

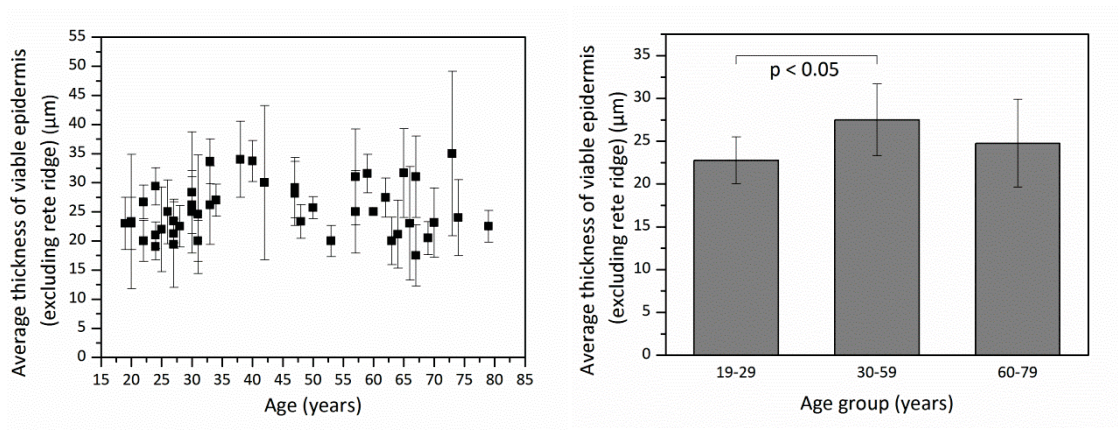


Fig. 7. Average thickness of viable epidermis (excluding rete ridge) versus age from the ventral forearms of 47 Asian subjects (skin phototype III & IV). In linear regression analysis, P-value for age = 0.3614 (not statistically significant); P-value for gender = 0.5475 (not statistically significant). In ANOVA, p-value for age group = 0.0107 (statistically significant); p-value for gender = 0.8920 (not statistically significant).

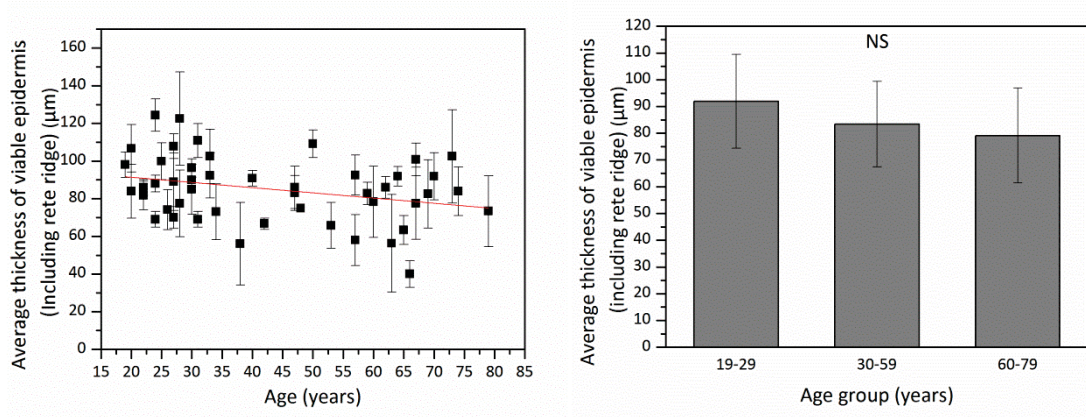


Fig. 8. Average thickness of viable epidermis (including rete ridge) versus age from the ventral forearms of 47 Asian subjects (skin phototype III & IV). In linear regression analysis, P-value for age = 0.0487 (statistically significant); P-value for gender = 0.3396 (not statistically significant). Correlation coefficient R to age = -0.293. In ANOVA, p-value for age group = 0.1592 (not statistically significant); p-value for gender = 0.4282 (not statistically significant). NS: not significant.

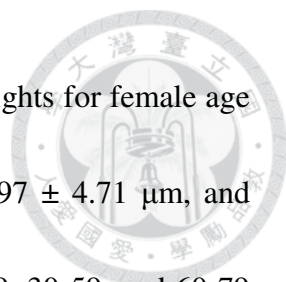


### 3.3 *In Vivo* Analysis of Isolated Dermal Papilla



#### 3.3.1 Height of Isolated Dermal Papilla

ANOVA showed statistical significances of age group for the three height parameters, average, intra-subject standard deviation, and maximum of height, respectively (Fig. 9-11; for age group,  $p_{ave} = 0.0003$ ,  $p_{SD} = 0.0051$ , and  $p_{max} = 0.0021$ ), but no significances of gender were found (Fig. 9-11; for gender,  $p_{ave} = 0.0975$ ,  $p_{SD} = 0.7703$ , and  $p_{max} = 0.5943$ ). Regression analysis also showed significances between age and the three height parameters, average, intra-subject standard deviation, and maximum of height (Fig. 9-11; for age,  $P_{ave} = 0.0003$ ,  $P_{SD} = 8.315 \times 10^{-5}$ , and  $P_{max} = 5.077 \times 10^{-5}$ ), respectively, but gender only showed significances in the regression analysis of the average height (for gender,  $P_{ave} = 0.0285$ ,  $P_{SD} = 0.4806$ , and  $P_{max} = 0.3165$ ). The intra-subject SD and the maximum of isolated dermal papilla height were negatively and moderately correlated only to age ( $R_{SD} = -0.540$ ;  $R_{max} = -0.551$ ). The average of isolated dermal papilla height was negatively and moderately correlated to both age and gender ( $R_{ave} = -0.563$ ). The overall average for male subjects of the average height ( $18.91 \mu\text{m}$ ) was higher than that for female subjects ( $15.54 \mu\text{m}$ ). The average heights for age groups 19-29, 30-59, and 60-79 years were  $21.90 \pm 5.98 \mu\text{m}$ ,  $15.01 \pm 4.85 \mu\text{m}$ , and  $14.25 \pm 4.11$



$\mu\text{m}$ . For respective age groups of females and males, the average heights for female age groups 19-29, 30-59, and 60-79 years were  $19.02 \pm 4.77 \mu\text{m}$ ,  $14.97 \pm 4.71 \mu\text{m}$ , and  $13.40 \pm 3.88 \mu\text{m}$ , and the average heights for male age groups 19-29, 30-59, and 60-79 years were  $24.41 \pm 6.06 \mu\text{m}$ ,  $15.10 \pm 5.61 \mu\text{m}$ , and  $15.38 \pm 4.47 \mu\text{m}$ . The intra-subject SDs of height for age groups 19-29, 30-59, and 60-79 years were  $11.76 \pm 4.37 \mu\text{m}$ ,  $8.10 \pm 5.14 \mu\text{m}$ , and  $6.21 \pm 2.69 \mu\text{m}$ . The maximum heights for subjects aged 19-29, 30-59, and 60-79 years were  $40.14 \pm 11.30 \mu\text{m}$ ,  $28.69 \pm 13.78 \mu\text{m}$ , and  $23.98 \pm 8.24 \mu\text{m}$ .

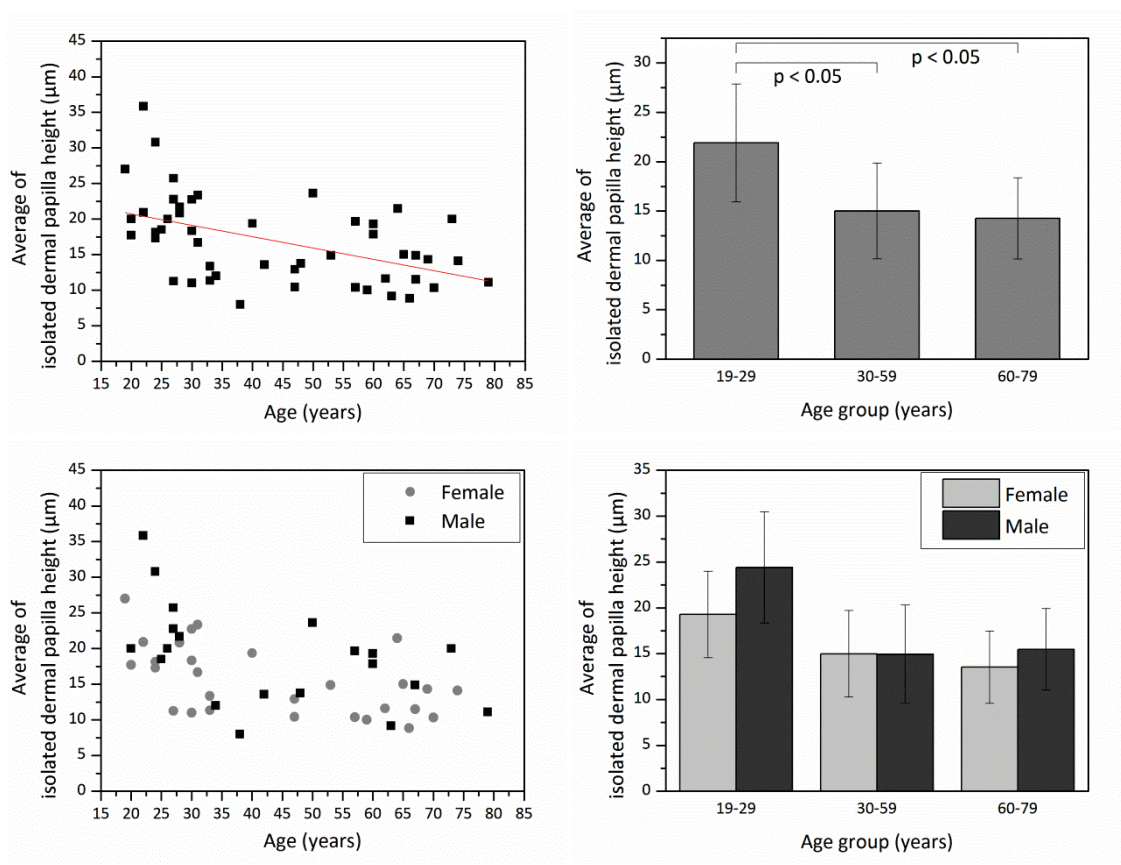


Fig. 9. Average of isolated dermal papilla height versus age from the ventral forearms of 48 Asian subjects (skin phototype III & IV). In linear regression analysis, P-value for age = 0.0003 (statistically significant); P-value for gender = 0.0285 (statistically significant). Correlation coefficient R to age and gender = -0.563.

In ANOVA, p-value for age group = 0.0003 (statistically significant); p-value for gender = 0.0975 (not statistically significant). In two lower figures, data of female and male subjects were separately displayed.

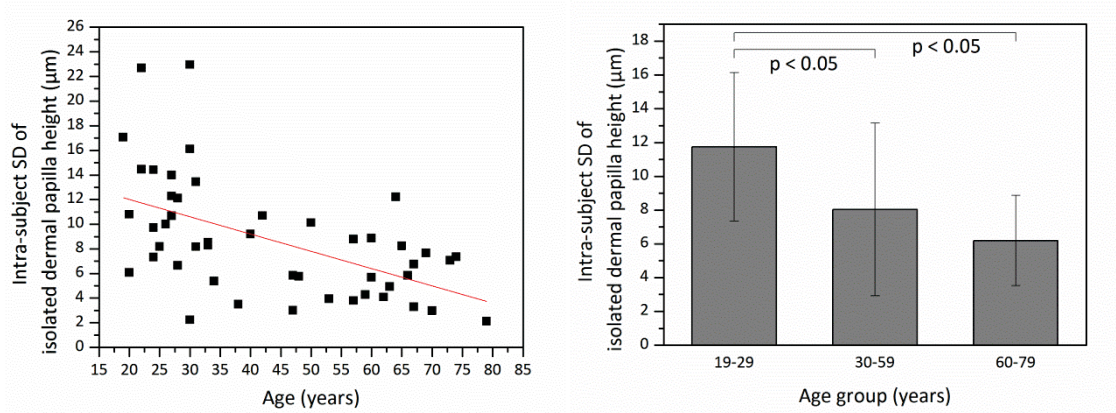


Fig. 10. Intra-subject standard deviation of isolated dermal papilla height versus age from the ventral forearms of 48 Asian subjects (skin phototype III & IV). In linear regression analysis, P-value for age =  $8.315 \times 10^{-5}$  (statistically significant); P-value for gender = 0.4806 (not statistically significant). Correlation coefficient R to age = -0.540. In ANOVA, p-value for age group = 0.0051 (statistically significant); p-value for gender = 0.7703 (not statistically significant).

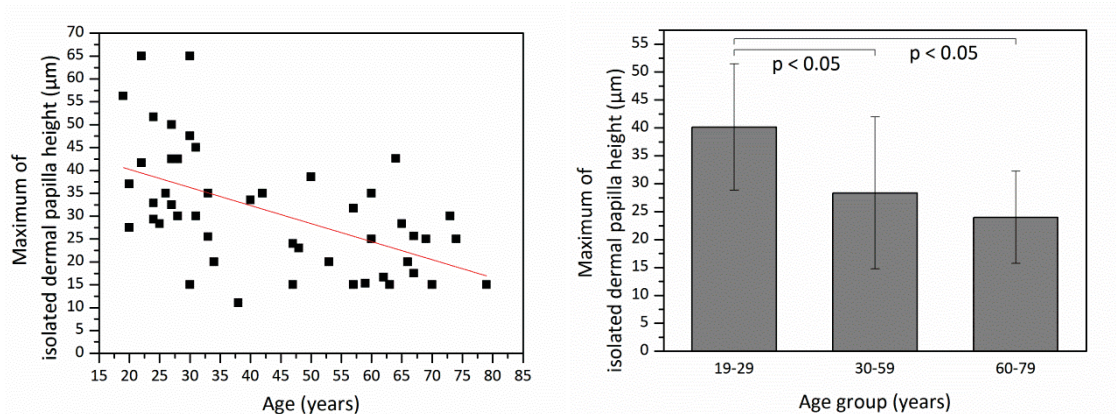


Fig. 11. Maximum of isolated dermal papilla height versus age from the ventral forearms of 48 Asian subjects (skin phototype III & IV). In linear regression analysis, P-value for age =  $5.077 \times 10^{-5}$  (statistically significant); P-value for gender = 0.3165 (not statistically significant). Correlation coefficient R to age = -0.551. In ANOVA, p-value for age group = 0.0021 (statistically significant); p-value for gender = 0.5943 (not statistically significant).



### 3.3.2 Volume of Isolated Dermal Papilla

ANOVA showed statistical significances of age group for the three volume parameters, average, intra-subject standard deviation, and maximum of volume, respectively (Fig. 12-14; for age group,  $p_{ave} = 0.0128$ ,  $p_{SD} = 0.0192$ , and  $p_{max} = 0.0067$ ), but no significances of gender were found (for gender,  $p_{ave} = 0.1604$ ,  $p_{SD} = 0.7484$ , and  $p_{max} = 0.4859$ ). There were statistical significances in the respective regression analyses of age and the three volume parameters, average, intra-subject standard deviation, and maximum of volume (Fig. 12-14; for age,  $P_{ave} = 0.0037$ ,  $P_{SD} = 0.0006$ , and  $P_{max} = 0.0005$ ). The average, intra-subject SD, and maximum of isolated dermal papilla volume were negatively related to age ( $R_{ave} = -0.405$ ;  $R_{SD} = -0.482$ ;  $R_{max} = -0.482$ ). In addition, we found that none of them were correlated to gender with statistical significances (for gender,  $P_{ave} = 0.0930$ ,  $P_{SD} = 0.5912$ , and  $P_{max} = 0.3244$ ). The average volumes for age groups 19-29, 30-59, and 60-79 years were  $45667 \pm 27010 \mu\text{m}^3$ ,  $27147 \pm 20758 \mu\text{m}^3$ , and  $24291 \pm 10794 \mu\text{m}^3$ . The intra-subject SDs of volume for age groups 19-29, 30-59, and 60-79 years were  $49776 \pm 28917 \mu\text{m}^3$ ,  $33155 \pm 30822 \mu\text{m}^3$ , and  $21219 \pm 9538 \mu\text{m}^3$ . The maximum volumes for age groups 19-29, 30-59, and 60-79 years were  $135624 \pm 80970 \mu\text{m}^3$ ,  $83118 \pm 68373 \mu\text{m}^3$ , and  $58694 \pm 23695 \mu\text{m}^3$ .

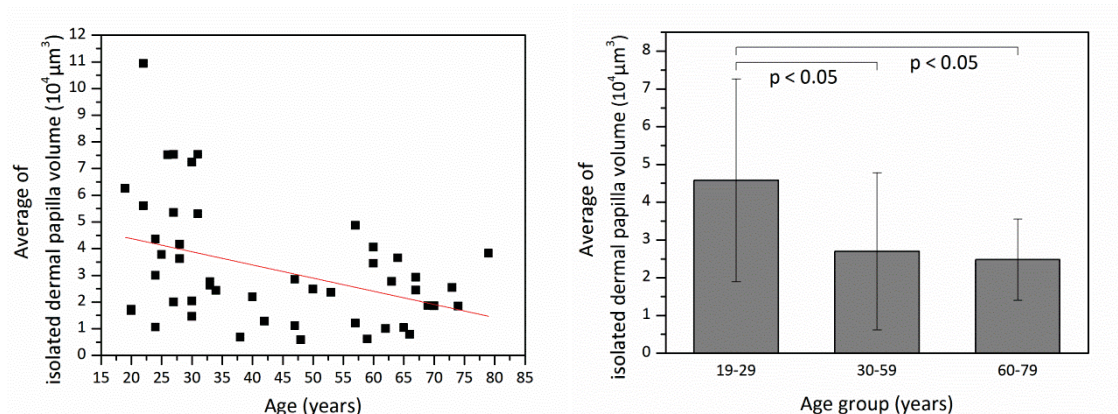


Fig. 12. Average of isolated dermal papilla volume versus age from the ventral forearms of 48 Asian subjects (skin phototype III & IV). In linear regression analysis, P-value for age = 0.0037 (statistically significant); P-value for gender = 0.0930 (not statistically significant). Correlation coefficient R to age = -0.405. In ANOVA, p-value for age group = 0.0128 (statistically significant); p-value for gender = 0.1604 (not statistically significant).

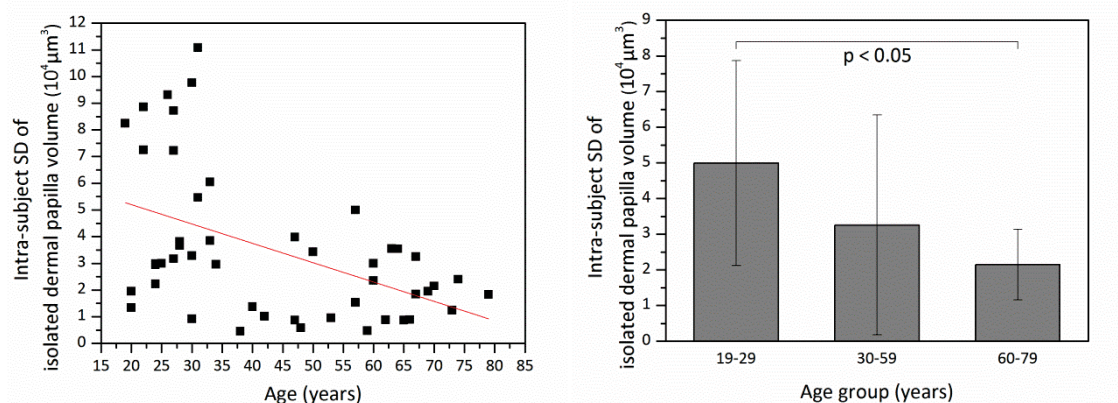


Fig. 13. Intra-subject SD of isolated dermal papilla volume versus age from the ventral forearms of 48 Asian subjects (skin phototype III & IV). In linear regression analysis, P-value for age = 0.0006 (statistically significant); P-value for gender = 0.5912 (not statistically significant). Correlation coefficient R to age = -0.482. In ANOVA, p-value for age group = 0.0192 (statistically significant); p-value for gender = 0.7484 (not statistically significant).

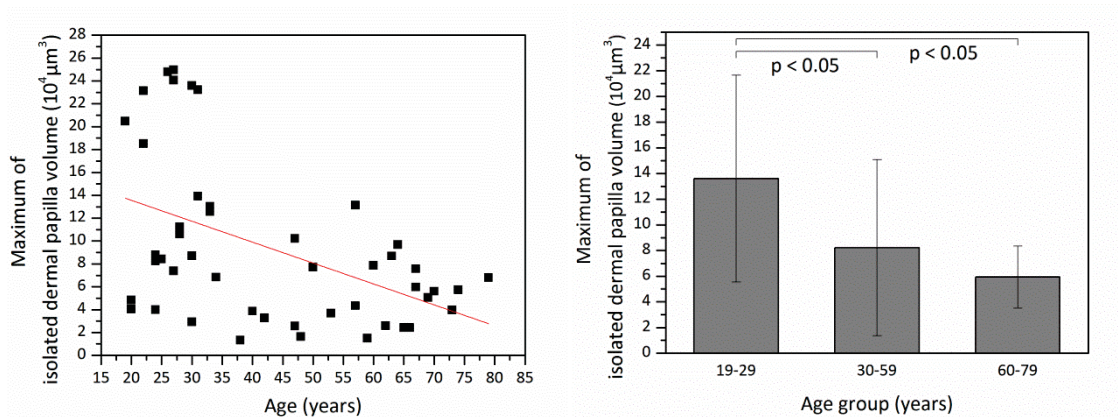


Fig. 14. Maximum of isolated dermal papilla volume versus age from the ventral forearms of 48 Asian subjects (skin phototype III & IV). In linear regression analysis, P-value for age = 0.0005 (statistically significant); P-value for gender = 0.3244 (not statistically significant). Correlation coefficient R to age = -0.482. In ANOVA, p-value for age group = 0.0067 (statistically significant); p-value for gender = 0.4859 (not statistically significant).

### 3.4 *In Vivo* Analysis of Dermal Papillae within Dermal Papilla Zone

#### 3.4.1 Depth of Dermal Papilla Zone

ANOVA of the depth of dermal papilla zone ( $T_{DPZ}$ ) only showed the statistical significance of age group (Fig. 15; p for age group = 0.0095 and p for gender = 0.2017).

The regression analysis was also statistically significant for age but not for gender (Fig.

15; P for age = 0.0009 and P for gender = 0.0989). The correlation was negative (R = -0.457) for the depth of dermal papilla zone to age. The depths for age groups 19-29,

30-59, and 60-79 years were  $74.22 \pm 13.25 \mu\text{m}$ ,  $60.63 \pm 16.32 \mu\text{m}$ , and  $57.20 \pm 14.29$



$\mu\text{m}$ . The result of thinner dermal papilla zone in the aged skin indicated that the dermal-epidermal junction flattened with aging.

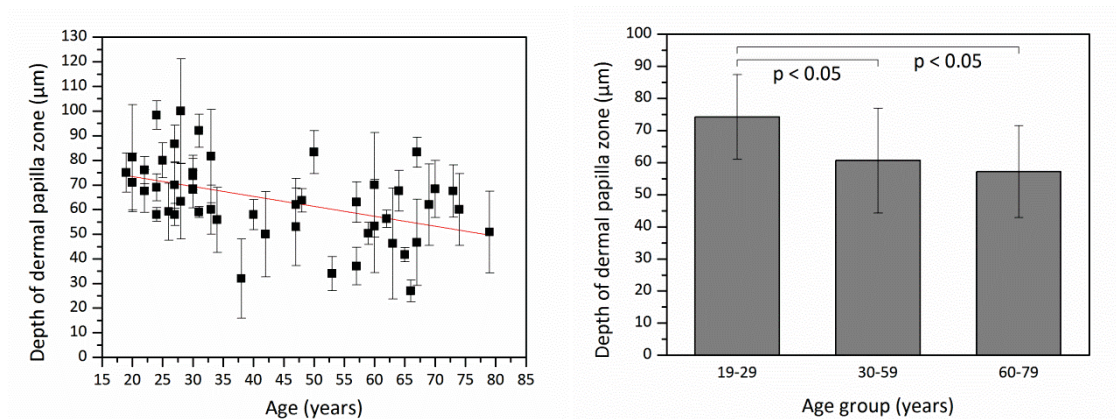
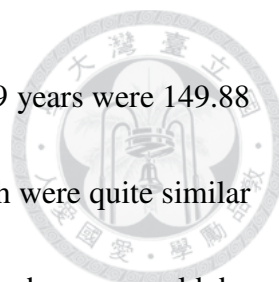


Fig. 15. Depth of dermal papilla zone versus age from the ventral forearms of 48 Asian subjects (skin phototype III & IV). In linear regression analysis, P-value for age = 0.0009 (statistically significant); P-value for gender = 0.0989 (not statistically significant). Correlation coefficient R to age = -0.457. In ANOVA, p-value for age group = 0.0095 (statistically significant); p-value for gender = 0.2017 (not statistically significant).

### 3.4.2 Number Density of Dermal Papillae

No statistical significance of age group nor gender was found in ANOVA of the number density of dermal papillae ( $D_N$ ; Fig. 16; p for age group = 0.8096 and p for gender = 0.3678). Similarly, the regression analysis showed no statistical significance for the number density of dermal papillae to age or gender (Fig. 16; P for age = 0.9503 and P for gender = 0.4749). Dermal papillae were not found to be more or fewer with increasing age. The average and inter-subject standard deviation of number density from all the subjects were  $148.65 \text{ mm}^{-2}$  and  $52.06 \text{ mm}^{-2}$ , and the coefficient of variance was



0.3502. The number densities for age groups 19-29, 30-59, and 60-79 years were  $149.88 \pm 55.07 \text{ mm}^{-2}$ ,  $149.54 \pm 49.58 \text{ mm}^{-2}$ , and  $146.14 \pm 55.85 \text{ mm}^{-2}$ , which were quite similar for different age groups. In Fig. 16, no tendency of age-related changes could be observed, and data were scattered in all age groups.

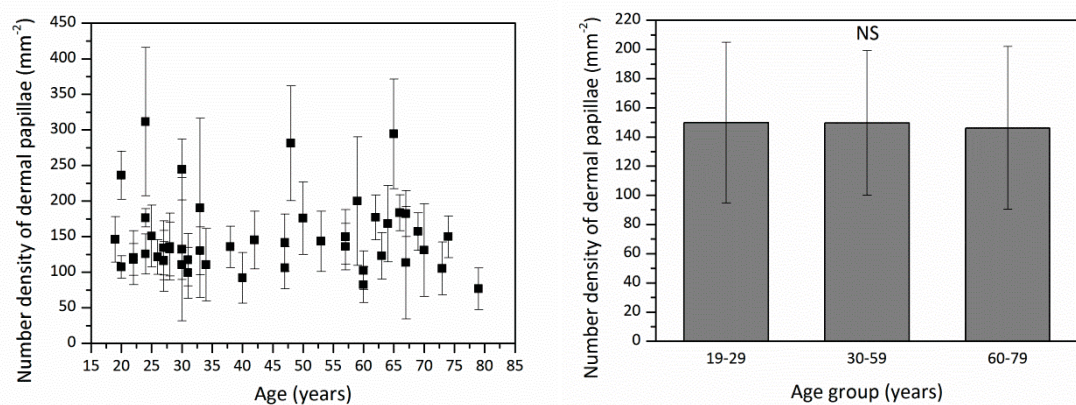
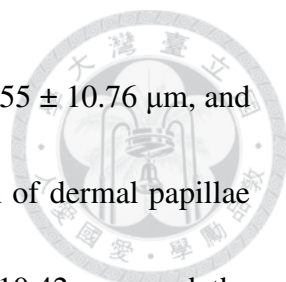


Fig. 16. Number density of dermal papillae versus age from the ventral forearms of 48 Asian subjects (skin phototype III & IV). In linear regression analysis, P-value for age = 0.9503 (not statistically significant); P-value for gender = 0.4749 (not statistically significant). In ANOVA, p-value for age group = 0.8096 (not statistically significant); p-value for gender = 0.3678 (not statistically significant). NS: not significant.

### 3.4.3 Dermal Papillae Volume per Unit Area

ANOVA of dermal papillae volume per unit area ( $D_V$ ) did not show statistical significances of age group and gender (Fig. 17; p for age group = 0.4008 and p for gender = 0.1561). There were no statistical significances in the regression analysis of dermal papillae volume per unit area to age and gender (Fig. 17; P for age = 0.1471 and P for gender = 0.1287). Therefore, the volume of dermal papillae within dermal papilla zone per unit area did not increase or decrease with age. The volumes per unit area for





age groups 19-29, 30-59, and 60-79 years were  $39.09 \pm 8.12 \mu\text{m}$ ,  $34.55 \pm 10.76 \mu\text{m}$ , and  $34.55 \pm 12.04 \mu\text{m}$ . The average and inter-subject standard deviation of dermal papillae volume per unit area from all the subjects were  $35.97 \mu\text{m}$  and  $10.42 \mu\text{m}$ , and the coefficient of variance was 0.2897. In Fig. 17, no tendency of increasing or decreasing with age could be observed, and data were scattered especially in elder groups.

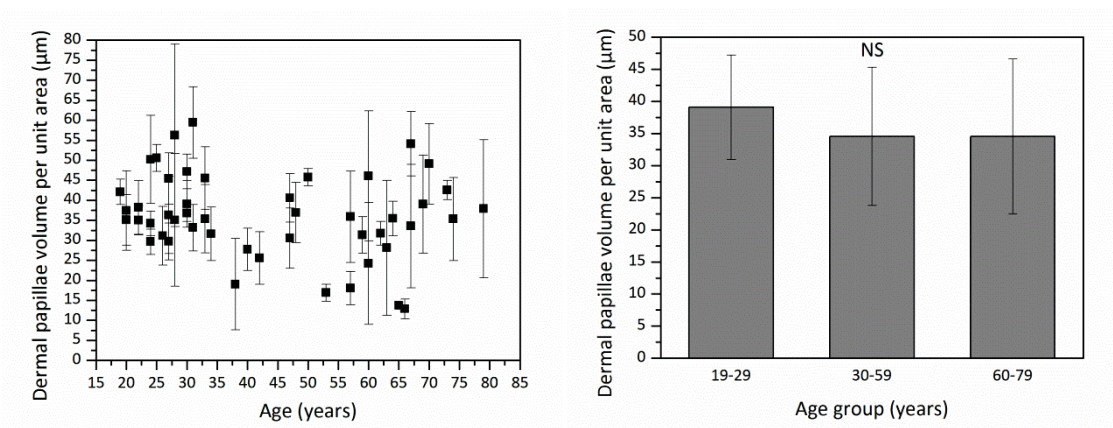


Fig. 17. Dermal papillae volume per unit area versus age from the ventral forearms of 48 Asian subjects (skin phototype III & IV). In linear regression analysis, P-value for age = 0.1471 (not statistically significant); P-value for gender = 0.1287 (not statistically significant). In ANOVA, p-value for age group = 0.4008 (not statistically significant); p-value for gender = 0.1561 (not statistically significant). NS: not significant.



### 3.4.4 Average Volume per Dermal Papilla

In ANOVA of the average volume per dermal papilla ( $V_{DP}$ ), effects of age group and gender were not statistically significant (Fig. 18;  $p$  for age group = 0.3120 and  $p$  for gender = 0.0920). In the same way, no statistical significances of age and gender were found in the regression analysis (Fig. 18;  $P$  for age = 0.5962 and  $P$  for gender = 0.1276). The average volumes per dermal papilla for age groups 19-29, 30-59, and 60-79 years were  $282387 \pm 80801 \mu\text{m}^3$ ,  $248257 \pm 100742 \mu\text{m}^3$ , and  $273554 \pm 129590 \mu\text{m}^3$ . The average and inter-subject standard deviation of average volume per dermal papilla from all the subjects were  $266301 \mu\text{m}^3$  and  $103472 \mu\text{m}^3$ , and the coefficient of variance was 0.3886. Therefore, if the connected part of a dermal papilla was included in the volume measurement, the average volume per dermal papilla did not decrease with age, which was different from the decreasing volume with age in the analysis of isolated dermal papilla.

It could be noticed that the average volume per dermal papilla ( $V_{\text{total}} / N_{\text{total}}$ ) was the dermal papillae volume per unit area ( $V_{\text{total}} / OA_{\text{max}}$ ) divided by the number density of dermal papillae ( $N_{\text{total}} / OA_{\text{max}}$ ). The dermal papillae volume per unit area and the number density of dermal papillae were not change with age, so it was reasonable that



the average volume per dermal papilla was not found related to age.

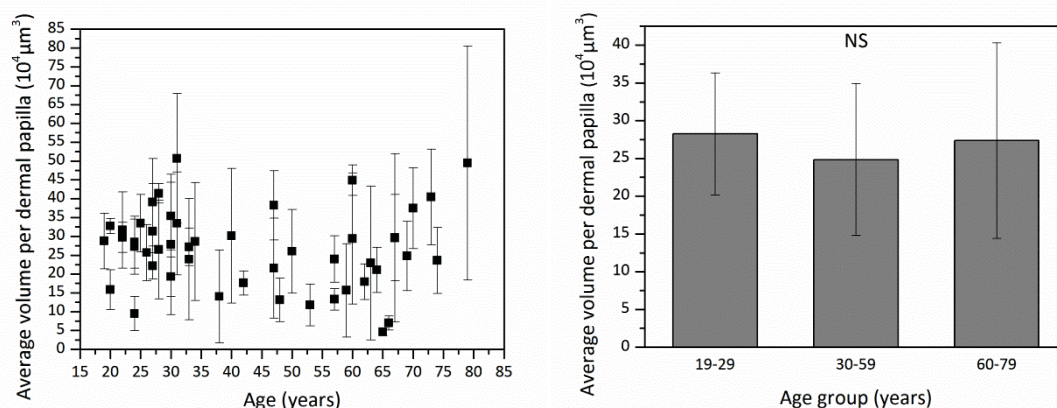
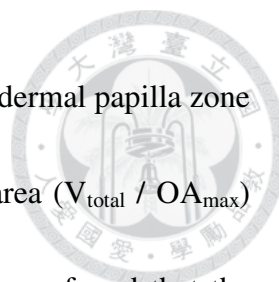


Fig. 18. Average volume per dermal papilla versus age from the ventral forearms of 48 Asian subjects (skin phototype III & IV). In linear regression analysis, P-value for age = 0.5962 (not statistically significant); P-value for gender = 0.1276 (not statistically significant). In ANOVA, p-value for age group = 0.3120 (not statistically significant); p-value for gender = 0.0920 (not statistically significant). NS: not significant.

### 3.4.5 Dermal Papillae Volume Ratio within Dermal Papilla Zone

ANOVA of the dermal papillae volume ratio within dermal papilla zone ( $R_V$ ) showed statistical significance of age group (Fig. 19; p for age group = 0.0423 and p for gender = 0.2307). We also found that the dermal papillae volume ratio within dermal papilla zone was positively correlated to age with the significance (Fig. 19; P for age = 0.0143 and P for gender = 0.3796;  $R = 0.352$ ). It meant that dermal papillae occupied more proportion of volume in the dermal papilla zone as age increased. The volume ratios for age groups 19-29, 30-59, and 60-79 years were  $52.46 \pm 4.26 \%$ ,  $56.26 \pm 5.49 \%$ , and  $59.18 \pm 11.34 \%$ .



It could be noticed that the dermal papillae volume ratio within dermal papilla zone ( $V_{total} / (OA_{max} \times T_{DPZ})$ ) was the dermal papillae volume per unit area ( $V_{total} / OA_{max}$ ) divided by the depth of dermal papilla zone ( $T_{DPZ}$ ). Previously, it was found that the dermal papillae volume per unit area was not related to age but the depth of dermal papilla zone decreased with increasing age, so the increase with age of the dermal papillae volume ratio within dermal papilla zone was quite reasonable.

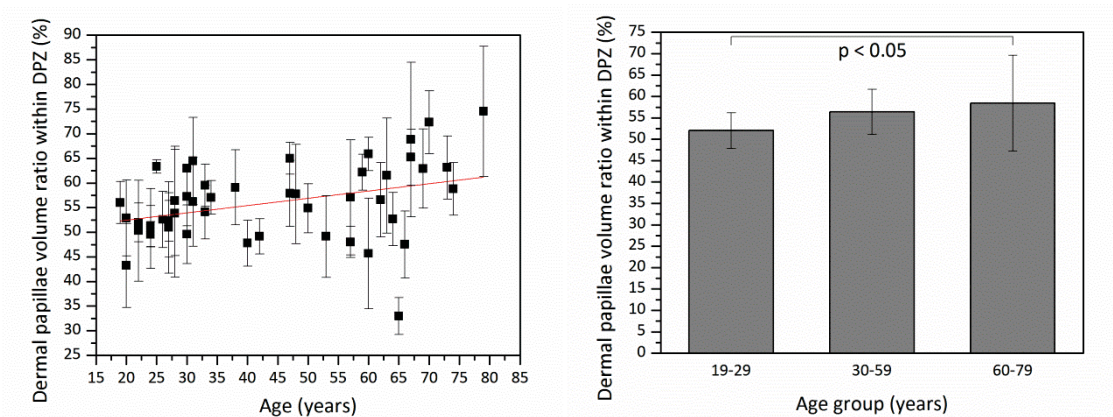


Fig. 19. Dermal papillae volume ratio within dermal papilla zone versus age from the ventral forearms of 48 Asian subjects (skin phototype III & IV). In linear regression analysis, P-value for age = 0.0143 (statistically significant); P-value for gender = 0.3796 (not statistically significant). Correlation coefficient R to age = 0.352. In ANOVA, p-value for age group = 0.0423 (statistically significant); p-value for gender = 0.2307 (not statistically significant).



### 3.4.6 3D Interdigitation Index

The statistical significance of age group was found in ANOVA of the 3D interdigitation index ( $I_{3D}$ ; Fig. 20;  $p$  for age group = 0.0013 and  $p$  for gender = 0.9041).

Similarly, it was showed that the correlation between the 3D interdigitation index and age was negative and moderate with statistical significance (Fig. 20;  $P$  for age =  $2.035 \times 10^{-5}$  and  $P$  for gender = 0.6453;  $R = -0.578$ ). The indexes for age groups 19-29, 30-59, and 60-79 years were  $2.734 \pm 0.378$ ,  $2.389 \pm 0.554$ , and  $2.089 \pm 0.291$ . The interface area of dermal papillae became smaller with advancing age, which revealed the undulation of dermal-epidermal junction was smaller in the older skin.

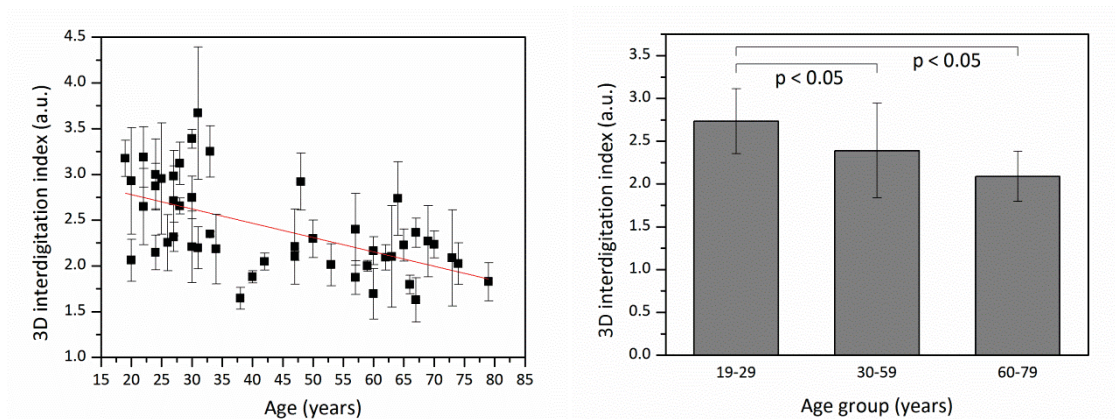


Fig. 20. 3D interdigitation index versus age from the ventral forearms of 48 Asian subjects (skin phototype III & IV). In linear regression analysis,  $P$ -value for age =  $2.035 \times 10^{-5}$  (statistically significant);  $P$ -value for gender = 0.6453 (not statistically significant). Correlation coefficient  $R$  to age =  $-0.578$ . In ANOVA,  $p$ -value for age group = 0.0013 (statistically significant);  $p$ -value for gender = 0.9041 (not statistically significant).

## Chapter 4 Discussion



### 4.1 Overall Results of *In Vivo* Aging Analysis

In this study, 10 of total 14 parameters were found to be related to age, and only 1 parameter was found to be related to gender. In the *in vivo* analysis of viable epidermis thickness, the thickness excluding the depth of rete ridge was not found to be related to age nor gender, but the thickness including the depth of rete ridge was negatively related to age. The results of the *in vivo* analysis of isolated dermal papilla showed that the average, the intra-subject standard deviation, and the maximum of isolated dermal papilla height and the average, the intra-subject standard deviation, and the maximum of isolated dermal papilla volume were all negatively related to age. Besides, the average of isolated dermal papilla height was larger for the male subjects. In the *in vivo* analysis of dermal papillae within dermal papilla zone, it was found that the depth of dermal papilla zone and the 3D interdigitation index were negatively related to age. On the contrary, the dermal papillae volume ratio within dermal papilla zone increased with increasing age. In addition, the number density of dermal papillae, the dermal papillae volume per unit area, and the average volume per dermal papilla was not found to be related to age nor gender.



## 4.2 Comparisons of Previous Studies

In the literature, some parameters have already been measured and their relations to intrinsic aging have been also studied.


### 4.2.1 Comparison between Results of Depth of Dermal Papilla Zone

It was found in the study of Neerken *et al.* that the depth of dermal papilla zone of volar forearm from 30 Caucasian volunteers showed a considerable decrease with increasing age by confocal laser scanning microscopy [31]. The analysis of this study also showed the decrease with increasing age for the Asian volunteers.

### 4.2.2 Comparison between Results of 3D Interdigitation Index

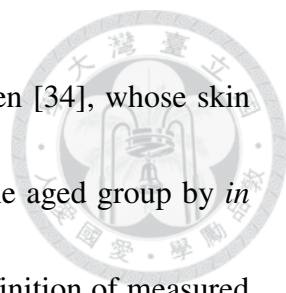
In the study of Timár *et al.*, it was found that the decrease of interdigitation index in the older inner forearm skin was significant by biopsy, which resulted from the interdigitation between the epidermis and the dermis disappearing related to intrinsic aging [30]. A similar age-related decrease was also found in the analysis of 3D interdigitation index, although the dimensions of measurements were different. Furthermore, the disappearance of interdigitation could be confirmed by the result that the depth of dermal papilla zone was decreasing with advancing age.

### 4.2.3 Comparison between Results of Viable Epidermis Thickness



In previous studies, many have studied the epidermis thickness repeatedly for several body sites by biopsy and *in vivo* techniques. However, the thickness of viable epidermis was measured in only a few studies or was studied indirectly, that is, measuring both stratum corneum and full epidermis to acquire the age-related change of viable epidermis. Due to the undulation of dermal-epidermal junction, the confirmation of whether the measurements included the rete ridge or not was required. Sandby-Møller *et al.* reported that the viable epidermis thickness of the dorsal forearm from 71 volunteers of different skin phototypes was independent of age by biopsy, and they claimed the sunlight exposure was negligible in the late autumn of Denmark [32]. They also reported that males had thicker viable epidermis than females, but it was not consistent with the result of this analysis. However, the definition of measurement was not given, so it could not be used as a reference of age effect. In the study of Koehler *et al.*, the viable epidermis thickness of the dorsal forearm from 30 volunteers, whose skin phototypes were not mentioned, was not found different between age groups by *in vivo* multiphoton laser tomography [33]. Nevertheless, they split the images into  $20\ \mu\text{m} \times 20\ \mu\text{m}$  and measured the thickness in a tiny field of view. To my knowledge, it was a mix of the measurements including and excluding rete ridge. Batisse *et al.* concluded that the






thickness of viable epidermis of the back of the arm from 34 women [34], whose skin phototypes were not mentioned, showed a significant decrease in the aged group by *in vivo* confocal microscopy and ultrasound imaging. However, the definition of measured region was not mentioned.

In this study, from both the measurements of viable epidermis thickness, I deduced that not the viable epidermis itself but the depth of rete ridge decreased in the aged skin. My conclusion was especially consistent with the conclusion made by Neerken *et al.* [31], who measured the full epidermis thicknesses excluding and including rete ridge separately of the volar forearm from 30 Caucasian volunteers by confocal laser scanning microscopy.

#### **4.2.4 Comparison between Results of Number Density of Dermal Papillae**

In the analysis of number density of dermal papillae, the inconsistency with previous studies was found. It was reported that the number of dermal papillae was significantly decreased in the aged forearm skin by several studies [31, 35-37]. To confirm the comparability of these studies, there were several details needed to be inspected.

First, the protocols of how to measure the number of dermal papillae, how to define



an individual papilla, and how to count the incomplete part were important. For the protocols of measurement, Sauermann *et al.* counted papillae in every frame of an image stack [35], and Koehler *et al.* counted papillae in only one depth that they located for imaging papillary dermis without detailed descriptions of depth [36]. Lagarrigue *et al.* counted full papillae observed in an image stack [37], and no details similar to the above mentioned were noted by Neerken *et al.* [31]. For the definition of an individual dermal papilla, only Sauermann *et al.* [35] mentioned that they defined the appearance of capillary as the criterion, and no definitions were mentioned by others. No descriptions of how to count the incomplete part were mentioned in these studies. It should be noted that no direct observation of dermis were made by Sauermann *et al.* and Lagarrigue *et al.*, and in confocal laser scanning microscopy images of Neerken *et al.*, epidermis and dermis could not be differentiated clearly as in our second- and third-harmonic generation images.

Second, the skin phototype was reported to influence the number of dermal papillae [37]. Skin phototypes in the study of Sauermann *et al.* were I to III mixed together, and Skin phototypes in the studies of Koehler *et al.* and Neerken *et al.* were believed to be I and II [31, 35, 36]. Lagarrigue *et al.* set skin phototype as one of the variables in the multiple regression analysis, and the decreases with age were observed for different skin

phototypes [37]. If subjects of many skin phototypes were included, skin phototypes should be taken as a variable to prevent incorrect deduction.



In my study, the number of dermal papillae was measured by counting the isolated dermal papillae, which appeared to be the individual cross-sections in the upper papillary dermis. Besides, in some subjects, the cross-sections of some isolated dermal papillae appeared to be very small and quickly connected to others in deeper skin, though the cross-sections of the isolated dermal papillae in other subjects appeared to be larger and rounder (Fig. 21). This difference between subjects was not related to age and seemed to considerably affect the measurement. However, this difference between subjects was not mentioned in those studies.

Other parameters including height of isolated dermal papilla, volume of isolated dermal papilla, dermal papillae volume per unit area, average volume per dermal papilla, and dermal papillae volume ratio within dermal papilla zone were not found to be studied in literature to my knowledge. These parameters might provide some new methods and insights to inspect and clarify the changes related to intrinsic aging.

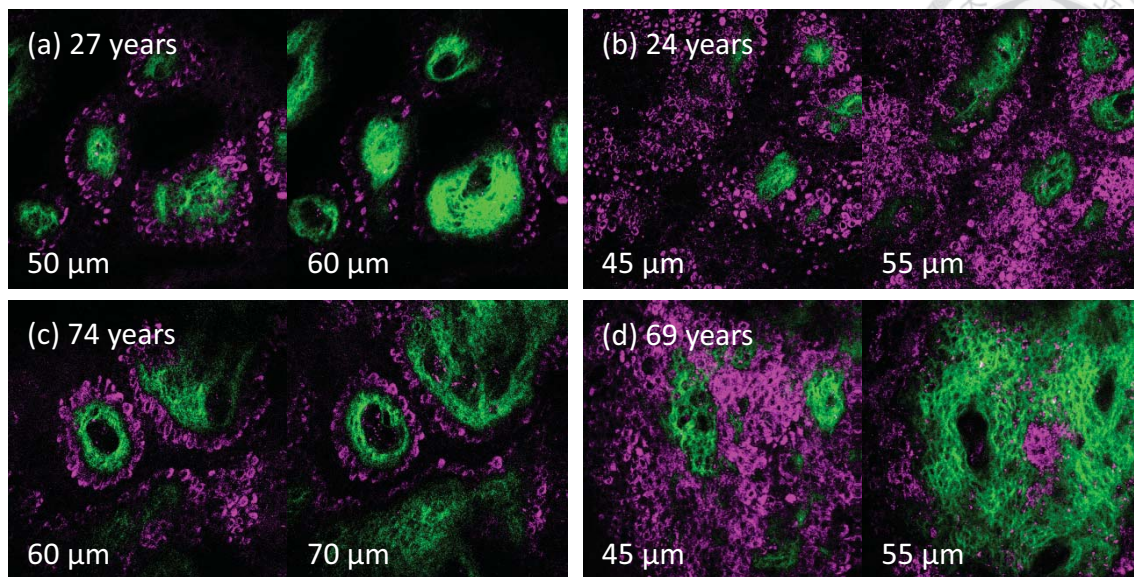


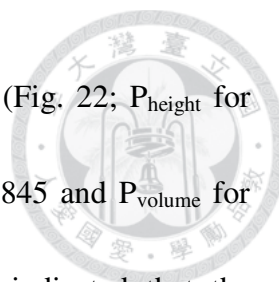
Fig. 21. Four sets of representative images from the ventral forearms of (a) 27-, (b) 24-, (c) 74-, and (d) 69-year-old subjects. The depths of images were labeled, and the depths of the first frames that showed the stratum corneum in respective stacks were set as 0  $\mu\text{m}$ . In (a) young and (c) elder skin, the cross-sections of isolated dermal papillae seemed to be larger and rounder; however, in other (b) young and (d) elder skin, the cross-sections of isolated dermal papillae appeared to be smaller and fragmentary. This difference between subjects did affect the number density of dermal papillae but was not related to age.

### 4.3 Deduction of Intrinsic Age-Related Changes of Skin

The analysis of the whole set of parameters combined together could provide several ways to comprehend the intrinsic age-related changes of the human skin. A deduction of the skin change related to age was addressed as the diagrams (Fig. 24 and 25), and details were described in the following paragraphs.

### 4.3.1 Deduction of Age-Related Changes of Isolated Dermal Papillae

In the *in vivo* analysis of isolated dermal papilla, the average, the intra-subject SD, and the maximum of isolated dermal papilla height and the average, the intra-subject SD, and the maximum of isolated dermal papilla volume were all decreasing with increasing age. The decreases of the maximums of height and volume showed that taller and bigger isolated dermal papillae diminished in the elder skin. Besides, the changes of the average height and volume indicate that the isolated dermal papillae as a whole became shorter and smaller. Furthermore, the decrease of the intra-subject standard deviation possibly implied that relatively larger isolated dermal papillae disappeared and the size of the isolated dermal papillae became similar. However, the size of each isolated dermal papilla might reduce with same proportion in the elder skin, and it would also make the average and the intra-subject SD decrease. In the foresaid condition, although the absolute value of intra-subject SD did decrease, the intra-subject SD relative to the average, which was the coefficient of variance, would not decreased at all. In that case, the decrease of intra-subject SD could not be interpreted as isolated dermal papillae becoming similar in size. To verify the foregoing possibility, the coefficients of variance of height and volume were calculated and analyzed by multiple linear regression analysis. It was found that both CVs of isolated dermal papilla height and volume were



negatively related to age with statistical significances respectively (Fig. 22;  $P_{\text{height}}$  for age = 0.0144 and  $P_{\text{volume}}$  for age = 0.0376;  $P_{\text{height}}$  for gender = 0.3845 and  $P_{\text{volume}}$  for gender = 0.1055;  $R_{\text{height}} = -0.352$  and  $R_{\text{volume}} = -0.295$ ), which indicated that the dispersions of the height and the volume were reduced in the older skin.

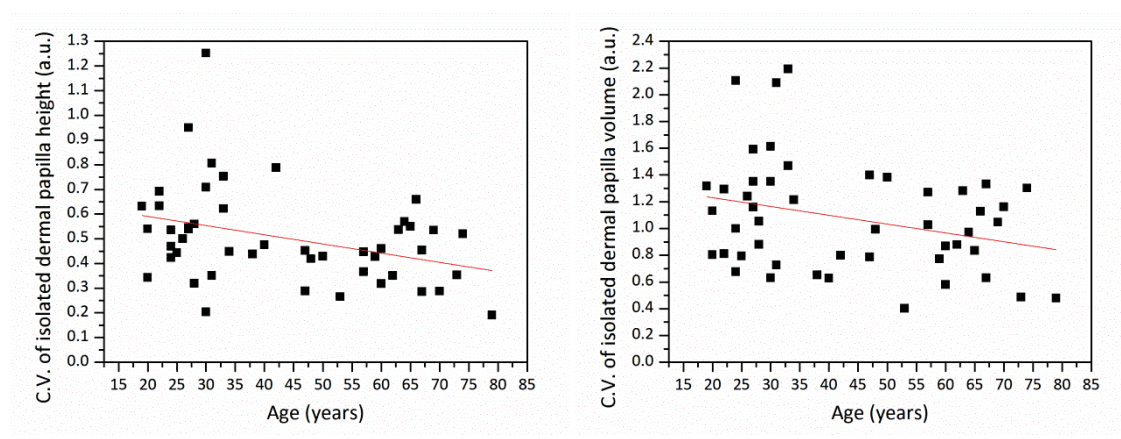


Fig. 22. Coefficient of variance of isolated dermal papilla height (left) versus age from the ventral forearms of 48 Asian subjects (skin phototype III & IV). In linear regression analysis, P-value for age = 0.0144 (statistically significant); P-value for gender = 0.3845 (not statistically significant). Correlation coefficient R to age = -0.352. Coefficient of variance of isolated dermal papilla volume (right) versus age from the ventral forearms of 48 Asian subjects (skin phototype III & IV). In linear regression analysis, P-value for age = 0.0376 (statistically significant); P-value for gender = 0.1055 (not statistically significant). Correlation coefficient R to age = -0.295.

To find out whether these isolated dermal papillae extended their widths with age or not, the average section area of isolated dermal papilla was calculated for each subject. For a subject, the respective section area of every his or her isolated dermal papilla was calculated by its volume divided by its height, and the average section area was acquired based on these section areas. The regression analysis did not show significance of age nor gender (Fig. 23; P for age = 0.6223 and P for gender = 0.1576),

so these isolated dermal papillae did not extend their widths with age.

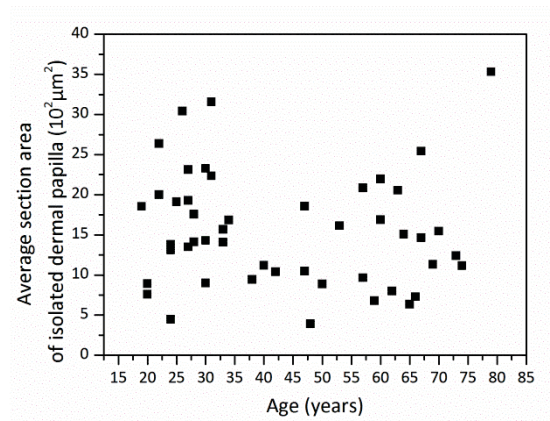


Fig. 23. Average section area of isolated dermal papilla versus age from the ventral forearms of 48 Asian subjects (skin phototype III & IV). In linear regression analysis, P-value for age = 0.6223 (not statistically significant); P-value for gender = 0.1576 (not statistically significant).

Therefore, the intrinsic aging resulted in the shrinkage of the isolated dermal papilla in size, which might reduce the interface area between dermis and epidermis, and the isolated dermal papilla did not extend or contract its width with age. Moreover, the analysis also indicated that both large and small isolated dermal papillae existed in the younger skin, but there were only small isolated dermal papillae remained in the elder skin (Fig. 24).

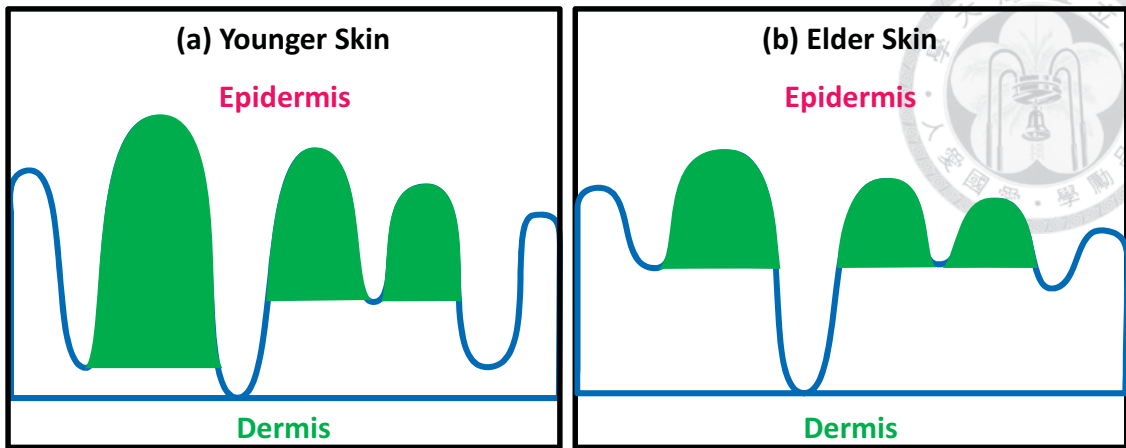


Fig. 24. Diagrams showed how isolated dermal papillae changed with aging. The isolated dermal papillae were shorter and smaller in the elder skin (b), and the sizes became similar. However, the isolated dermal papillae did not extend their widths in the elder skin.

### 4.3.2 Deduction of Age-Related Changes of Dermal Papillae within Dermal Papilla Zone

**Table 2. The summary of changes with increasing age of parameters in the analysis of dermal papillae within dermal papilla zone**

Parameters	$T_{DPZ}$	$D_N$	$D_V$	$V_{DP}$	$R_V$	$I_{3D}$
<b>Increase/Decrease with Increasing Age</b>	↓	×	×	×	↑	↓

×: Not increase or decrease with increasing age

In the *in vivo* analysis of dermal papillae within dermal papilla zone, the depth of dermal papilla zone ( $T_{DPZ}$ ), the dermal papillae volume ratio within dermal papilla zone ( $R_V$ ), and the 3D interdigitation index ( $I_{3D}$ ) were found to increase or decrease with age. However, the number density of dermal papillae ( $D_N$ ), the dermal papillae volume per





unit area ( $D_V$ ), and the average volume per dermal papillae ( $V_{DP}$ ) were not found increased or decreased with age.

First of all, the depth of dermal papilla zone became smaller in the aged skin, and the max occupied section area depended on how many stacks were analyzed and how much space of an image was occupied by the bottom of dermal papilla zone. The whole volume of dermal papilla zone thus decreased with age:

$\therefore T_{DPZ} \downarrow$  with age &  $OA_{max}$  is arbitrary,

$\therefore$  Volume of DPZ =  $(T_{DPZ} \times OA_{max}) \downarrow$  with age.

Secondly, the dermal papillae volume per unit area was not found increased or decreased with age. The dermal papillae volume ratio within dermal papilla zone increased and the depth of dermal papilla zone decreased with age. Because the volume ratio could be calculated from the volume per unit area divided by the depth, the increase of volume ratio with age simply resulted from the decrease of the depth with age:

$$D_V = \frac{V_{total}}{OA_{max}} \times \text{with age},$$

$R_V \uparrow$  with age &  $T_{DPZ} \downarrow$  with age,

$$\therefore R_V = \frac{V_{\text{total}}}{(OA_{\text{max}} \times T_{\text{DPZ}})} = \frac{D_V}{T_{\text{DPZ}}},$$

$$\therefore T_{\text{DPZ}} \downarrow \text{ with age} \Rightarrow R_V = \frac{D_V}{T_{\text{DPZ}}} \uparrow \text{ with age.}$$



With the same max occupied section area, the total volume of dermal papillae within dermal papilla zone could be considered consistent with increasing age:

$$D_V = \frac{V_{\text{total}}}{OA_{\text{max}}} \times \text{with age,}$$

$OA_{\text{max}}$  is arbitrary,

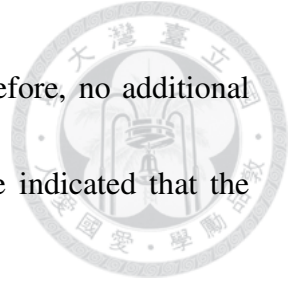
$$\therefore V_{\text{total}} \times \text{with age.}$$

While the dermal papilla zone became thinner with age, the dermal papillae within dermal papilla zone should extend their waistlines with the consistent volume:

$$\therefore T_{\text{DPZ}} \downarrow \ \& \ V_{\text{total}} \times \text{with age,}$$

$$\therefore \text{waistlines of DP} \uparrow \text{ with age.}$$

To show the waistline extension of the dermal papillae within dermal papilla zone, it might be suitable to calculate the average occupied section area of dermal papillae within dermal papilla zone, which was the total dermal papillae volume divided by the depth of dermal papilla zone. However, the average occupied section area equaled to the volume ratio multiplied by the max occupied section area, so the volume ratio could be



explained as the average occupied section area per unit area. Therefore, no additional calculation was needed, and the increase of volume ratio with age indicated that the average occupied section area increased with age:

$$OA_{ave} = \text{Average Occupied Section Area of DP within DPZ} = \frac{V_{total}}{T_{DPZ}},$$

$$\therefore R_V = \frac{V_{total}}{(OA_{max} \times T_{DPZ})}$$

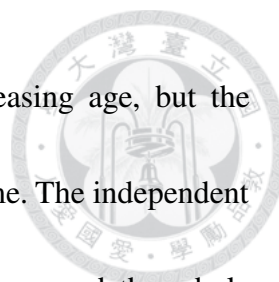
$$\therefore OA_{ave} = \frac{V_{total}}{T_{DPZ}} = R_V \times OA_{max} \Rightarrow R_V = \frac{OA_{ave}}{OA_{max}}.$$

$\therefore OA_{max}$  is arbitrary

$\therefore R_V \uparrow$  with age  $\Rightarrow OA_{ave} \uparrow$  with age.

However, it was found previously in 4.3.1 that the isolated dermal papillae did not extend their widths with age. Therefore, the independent dermal papillae should connect to each other quicker in the aged skin, and it was the whole dermal papillae within dermal papilla zone that extended in width and their occupied section area increased with age. In addition, the 3D interdigitation index was found to be smaller in the elder skin, and it indicated that the undulation of dermal papillae became smoother.

In summary, the number density of dermal papillae was not found related to age, and the differences between people were quite large. Moreover, the results of the



analysis indicated that dermal papilla zone was thinner with increasing age, but the dermal papillae within dermal papilla zone were not reduced in volume. The independent dermal papillae connected to each other quicker with increasing age, and the whole dermal papillae within dermal papilla zone extended in width. These age-related changes of dermal papillae were showed in Fig. 25, and 9 representative 3D reconstructions of image stacks, which displayed only dermal papillae within dermal papilla zone, were showed in Fig. 26.

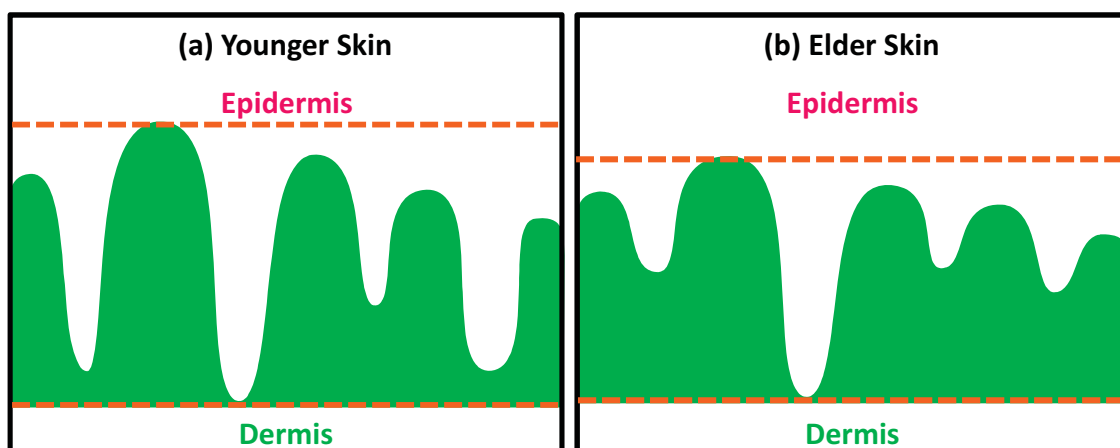


Fig. 25. Diagrams that showed how dermal papillae within dermal papilla zone changed with aging. In the elder skin, with the thinner dermal papilla zone, the dermal papillae within dermal papilla zone became shorter but extended in width and occupied more proportion of the volume of dermal papilla zone.

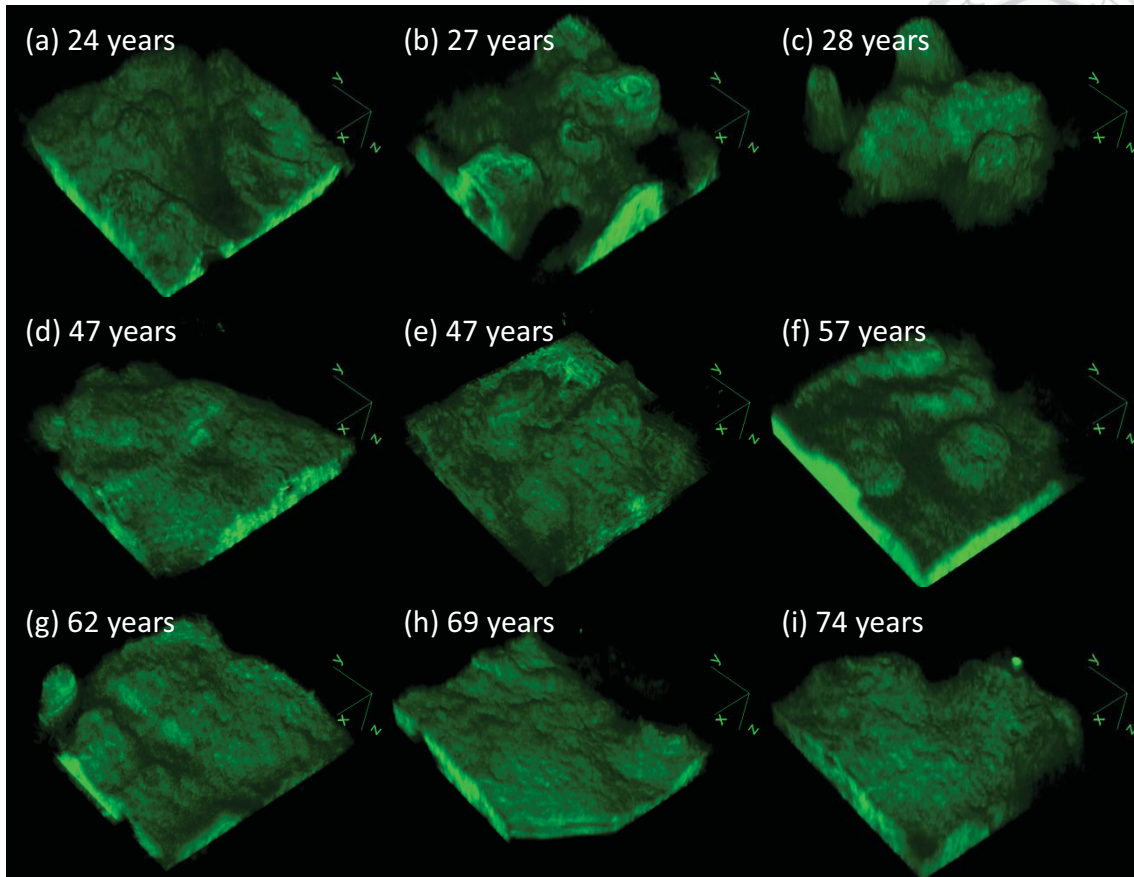



Fig. 26. 3D reconstructions of 9 XYZ image stacks from the ventral forearms of (a) 24-, (b) 27-, (c) 28-, (d) 47-, (e) 47-, (f) 57-, (g) 62-, (h) 69-, and (i) 74-year-old subjects. Only SHG signals within the dermal papilla zone were used in the 3D reconstructions, which revealed the structure of dermal papillae. In (d), (e), and (g), the step size between images was  $2\ \mu\text{m}$ , and the X-Y-Z dimensions of the 3D reconstructions were  $240\ \mu\text{m} \times 240\ \mu\text{m} \times 84\ \mu\text{m}$ . In the others, the step size was  $5\ \mu\text{m}$ , and the X-Y-Z dimensions were  $240\ \mu\text{m} \times 240\ \mu\text{m} \times 85\ \mu\text{m}$ . The coordinate axes were added beside the reconstructions, and z-axes pointed to the deeper dermis. The 3D reconstructions were built by ImageJ 3D Viewer.

**Table 3. Depth of DPZ, DP volume per unit area, DP volume ratio within DPZ, and 3D interdigitation index for each image stack in Fig. 26**

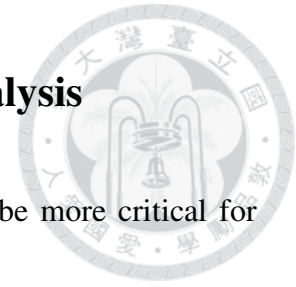
	$T_{\text{DPZ}}$	$D_v$	$R_v$	$I_{3\text{D}}$		$T_{\text{DPZ}}$	$D_v$	$R_v$	$I_{3\text{D}}$		$T_{\text{DPZ}}$	$D_v$	$R_v$	$I_{3\text{D}}$
(a)	70	38	0.54	2.25	(b)	80	38	0.48	2.95	(c)	85	40	0.47	2.96
(d)	66	41	0.62	2.68	(e)	64	33	0.51	2.16	(f)	65	40	0.62	2.51
(g)	52	35	0.67	1.94	(h)	55	33	0.60	1.96	(i)	65	43	0.66	2.07



Besides dermal papillae, the rest space of dermal papilla zone was occupied by rete ridge, which were downward protrusions of epidermis. By investigating age-related changes of dermal papillae, the relative changes of rete ridge could be understood. First, rete ridge became shorter as the dermal papilla zone became thinner with age. Besides, the isolated dermal papillae connected to each other quickly in the aged skin, so most rete ridge became much shorter. Furthermore, because the isolated dermal papillae did not extend their widths, the rete ridge would only become shorter but not slenderer.

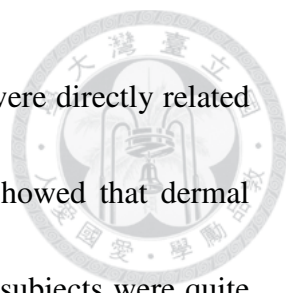
The major function of the dermal-epidermal junction was to attach the epidermis and dermis and reduce the risk of separation between these two layers [38]. Furthermore, for a unit area of the skin, the larger interface area of the dermal-epidermal junction for connecting these two layers, the stronger capability of preventing separation by external force. The 3D interdigitation index measured the interface area of the dermal-epidermal junction for a unit area of the skin, and the analysis revealed that the interface area became smaller with advancing age. It might imply that the fragility of the aged skin was possibly related to the decreased interface area of the dermal-epidermal junction, which weakened the strength of epidermal-dermal adherence.

## 4.4 Discussion of Critical Parameters in this Analysis



Among all these 14 parameters, some parameters seemed to be more critical for revealing the age-related changes of the human skin. Both measurements of viable epidermis thickness including and excluding rete ridge implied the flattened dermal-epidermal junction, but this indication could be obtained from direct measurement of the depth of dermal papilla zone. The analysis of the height and the volume of isolated dermal papilla provided the insight into the structure of upper-part dermal papillae and the definition for counting the number of dermal papilla. The decrease of height and volume might also indicate the decrease of the interface area of the dermal-epidermal junction, but the change of the interface area was better to be observed by measuring the full interface area. In short, the analysis of viable epidermis and isolated dermal papilla could only provide indirect biological meanings.

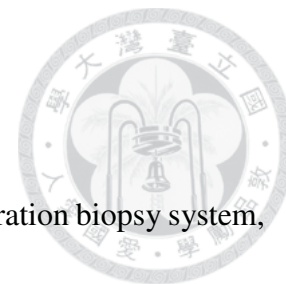
However, some insights could be provided by the analysis of dermal papillae within dermal papilla zone. The parameters in this analysis were related to each other and basically calculated by four independent features of the dermal papillae: number, depth, volume, and interface area. Therefore, the critical parameters were the four parameters, number density of dermal papillae, depth of dermal papilla zone, dermal



papillae volume per unit area, and 3D interdigitation index, which were directly related to four respective features. First, the analysis of number density showed that dermal papillae did not become less with age, and the differences between subjects were quite large, which was inconsistent with other studies. No tendency of decrease with age could be observed from the data (Fig. 16), which was supported by high p-values for age and age group in the regression analysis and ANOVA. Second, the decrease of the depth of dermal papilla zone directly showed that the dermal-epidermal junction flattened with age. Third, the observation of the dermal papillae volume per unit area could show whether the dermal papillae within dermal papilla zone diminished in volume with age or not, and the analysis showed that the dermal papillae volume per unit area were not affected by age. Finally, the decrease of the 3D interdigitation index with age showed that the decreased interface area of dermal-epidermal junction in the aged skin, which might weaken the capability to prevent the separation of epidermis and dermis.



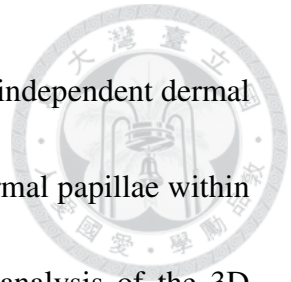
## Chapter 5 Conclusion



Using the XYZ image stacks acquired by *in vivo* harmonic generation biopsy system, 14 parameters were defined to inspect morphological changes of viable epidermis and mainly dermal papillae in a three-dimensional point of view. Among these parameters, 10 parameters were found to be related to age. Only 1 parameter was found related to gender. From the analysis of whole set of these parameters combined, the deduction of changes of skin was made to describe the overall effect of intrinsic aging (Fig. 24 and 25).

The results of the *in vivo* analysis of viable epidermis thickness implied the flattened dermal-epidermal junction in the aged skin. The results of the *in vivo* analysis of isolated dermal papilla indicated that the intrinsic aging resulted in the shrinkage of the isolated dermal papilla in size, which might reduce the interface area between dermis and epidermis, and the isolated dermal papilla did not extend its width with age. Moreover, the analysis also showed that both large and small isolated dermal papillae existed in the younger skin, but there were only small isolated dermal papillae remained in the elder skin (Fig. 24). The results of the *in vivo* analysis of dermal papillae within dermal papilla zone indicated the dermal papillae were not fewer in the aged skin. Furthermore, dermal papilla zone became thinner with increasing age, but the dermal

papillae within dermal papilla zone were not reduced in volume. The independent dermal papillae connected to each other quicker with age, and the whole dermal papillae within dermal papilla zone extended in width (Fig. 25). Moreover, the analysis of the 3D interdigitation index showed the decreasing interface area of the dermal-epidermal junction with age, which might related to the fragility of the aged skin due to the weakening of epidermal-dermal adherence.




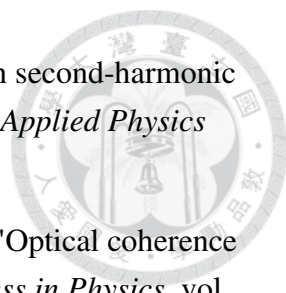
## Reference

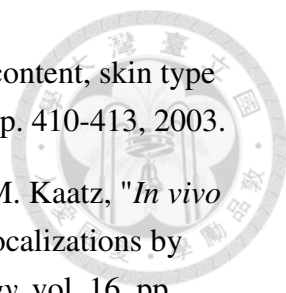


- [1] M. A. Farage, K. W. Miller, P. Elsner, and H. I. Maibach, "Intrinsic and extrinsic factors in skin ageing: A review," *International Journal of Cosmetic Science*, vol. 30, pp. 87-95, 2008.
- [2] B. A. Gilchrest, "Skin aging and photoaging: An overview," *Journal of the American Academy of Dermatology*, vol. 21, pp. 610-613, 1989.
- [3] A. M. Kligman and C. Koblenzer, "Demographics and psychological implications for the aging population," *Dermatologic Clinics*, pp. 549-553, 1997.
- [4] R. W. Boyd, *Nonlinear optics*. San Diego: Academic Press, 1992.
- [5] Y. Guo, P. P. Ho, A. Tirkšliunas, F. Liu, and R. R. Alfano, "Optical harmonic generation from animal tissues by the use of picosecond and femtosecond laser pulses," *Appl Opt*, vol. 35, pp. 6810-6813, 1996.
- [6] S. W. Chu, I. H. Chen, T. M. Liu, P. C. Chen, C. K. Sun, and B. L. Lin, "Multimodal nonlinear spectral microscopy based on a femtosecond Cr:forsterite laser," *Optics Letters*, vol. 26, pp. 1909-1911, 2001.
- [7] J. N. Gannaway and C. J. R. Sheppard, "Second-harmonic imaging in the scanning optical microscope," *Optical and Quantum Electronics*, vol. 10, pp. 435-439, 1978.
- [8] D. Yelin and Y. Silberberg, "Laser scanning third-harmonic-generation microscopy in biology," *Optics Express*, vol. 5, pp. 169-175, 1999.
- [9] S. W. Chu, S. Y. Chen, G. W. Chern, T. H. Tsai, Y. C. Chen, B. L. Lin, and C. K. Sun, "Studies of  $c^{(2)}/c^{(3)}$  tensors in submicron-scaled bio-tissues by polarization harmonics optical microscopy," *Biophysical Journal*, vol. 86, pp. 3914-3922, 2004.
- [10] E. Brown, T. McKee, E. diTomaso, A. Pluen, B. Seed, Y. Boucher, and R. K. Jain, "Dynamic imaging of collagen and its modulation in tumors *in vivo* using second-harmonic generation," *Nature Medicine*, vol. 9, pp. 796-800, 2003.
- [11] M. R. Tsai, Y. W. Chiu, M. T. Lo, and C. K. Sun, "Second-harmonic generation imaging of collagen fibers in myocardium for atrial fibrillation diagnosis,"

*Journal of Biomedical Optics*, vol. 15, p. 026002, 2010.

- 
- [12] T. Y. F. Tsang, "Optical third-harmonic generation at interfaces," *Physical Review A*, vol. 52, pp. 4116-4125, 1995.
- [13] D. Debarre, W. Supatto, A.-M. Pena, A. Fabre, T. Tordjmann, L. Combettes, M.-C. Schanne-Klein, and E. Beaurepaire, "Imaging lipid bodies in cells and tissues using third-harmonic generation microscopy," *Nature Methods*, vol. 3, pp. 47-53, 2006.
- [14] S. Y. Chen, S. U. Chen, H. Y. Wu, W. J. Lee, Y. H. Liao, and C. K. Sun, "In vivo virtual biopsy of human skin by using noninvasive higher harmonic generation microscopy," *IEEE Journal of Selected Topics in Quantum Electronics*, vol. 16, pp. 478-492, 2010.
- [15] C. F. Chang, C. H. Yu, and C. K. Sun, "Multi-photon resonance enhancement of third harmonic generation in human oxyhemoglobin and deoxyhemoglobin," *Journal of Biophotonics*, vol. 3, pp. 678-685, 2010.
- [16] C. K. Sun, C. H. Yu, S. P. Tai, C. T. Kung, I. J. Wang, H. C. Yu, H. J. Huang, W. J. Lee, and Y. F. Chan, "In vivo and ex vivo imaging of intra-tissue elastic fibers using third-harmonic-generation microscopy," *Optics Express*, vol. 15, pp. 11167-11177, 2007.
- [17] C. H. Yu, S. P. Tai, C. T. Kung, W. J. Lee, Y. F. Chan, H. L. Liu, J. Y. Lyu, and C. K. Sun, "Molecular third-harmonic-generation microscopy through resonance enhancement with absorbing dye," *Optics Letters*, vol. 33, pp. 387-389, 2008.
- [18] S. Y. Chen, H. Y. Wu, and C. K. Sun, "In vivo harmonic generation biopsy of human skin," *Journal of Biomedical Optics*, vol. 14, p. 060505, 2009.
- [19] B. E. Applegate, C. Yang, A. M. Rollins, and J. A. Izatt, "Polarization-resolved second-harmonic-generation optical coherence tomography in collagen," *Optics Letters*, vol. 29, pp. 2252-2254, 2004.
- [20] M. V. Sarunic, B. E. Applegate, and J. A. Izatt, "Spectral domain second-harmonic optical coherence tomography," *Optics Letters*, vol. 30, pp. 2391-2393, 2005.
- [21] Y. Jiang, I. Tomov, Y. Wang, and Z. Chen, "Second-harmonic optical coherence tomography," *Optics Letters*, vol. 29, pp. 1090-1092, 2004.

- 
- [22] Y. Jiang, I. V. Tomov, Y. Wang, and Z. Chen, "High-resolution second-harmonic optical coherence tomography of collagen in rat-tail tendon," *Applied Physics Letters*, vol. 86, p. 3901, 2005.
- [23] A. F. Fercher, W. Drexler, C. K. Hitzenberger, and T. Lasser, "Optical coherence tomography - principles and applications," *Reports on Progress in Physics*, vol. 66, p. 239, 2003.
- [24] K. König and I. Riemann, "High-resolution multiphoton tomography of human skin with subcellular spatial resolution and picosecond time resolution," *Journal of Biomedical Optics*, vol. 8, p. 432, 2003.
- [25] S. W. Chu, S. Y. Chen, T. H. Tsai, T. M. Liu, C. Y. Lin, H. J. Tsai, and C. K. Sun, "In vivo developmental biology study using noninvasive multi-harmonic generation microscopy," *Optics Express*, vol. 11, pp. 3093-3099, 2003.
- [26] S. Y. Chen, H. C. Yu, I. J. Wang, and C. K. Sun, "Infrared-based third and second harmonic generation imaging of cornea," *Journal of Biomedical Optics*, vol. 14, p. 044012, 2009.
- [27] R. R. Anderson and J. A. Parrish, "The optics of human skin," *Journal of Investigative Dermatology*, vol. 77, pp. 13-19, 1981.
- [28] C. C. Wang, "Chromium-doped forsterite laser mode-locking and its applications," Master, Graduate Institute of Photonics and Optoelectronics, National Taiwan University, Taipei, 1999.
- [29] S. H. Chia, T. M. Liu, A. A. Ivanov, A. B. Fedotov, A. M. Zheltikov, M. R. Tsai, M. C. Chan, C. H. Yu, and C. K. Sun, "A sub-100fs self-starting Cr:forsterite laser generating 1.4w output power," *Optics Express*, vol. 18, pp. 24085-24091, 2010.
- [30] F. Timár, G. Soos, B. Szende, and A. Horvath, "Interdigitation index - a parameter for differentiating between young and older skin specimens," *Skin Research and Technology*, vol. 6, pp. 17-20, 2000.
- [31] S. Neerken, G. W. Lucassen, M. A. Bisschop, E. Lenderink, and T. Nuijs, "Characterization of age-related effects in human skin: A comparative study that applies confocal laser scanning microscopy and optical coherence tomography," *Journal of Biomedical Optics*, vol. 9, pp. 274-281, 2004.
- [32] J. Sandby-Møller, T. Poulsen, and H. C. Wulf, "Epidermal thickness at different

- 
- body sites: Relationship to age, gender, pigmentation, blood content, skin type and smoking habits," *Acta Dermato-Venereologica*, vol. 83, pp. 410-413, 2003.
- [33] M. J. Koehler, T. Vogel, P. Elsner, K. König, R. Buckle, and M. Kaatz, "In vivo measurement of the human epidermal thickness in different localizations by multiphoton laser tomography," *Skin Research and Technology*, vol. 16, pp. 259-264, 2010.
- [34] D. Batisse, R. Bazin, T. Baldeweck, B. Querleux, and J.-L. Lévêque, "Influence of age on the wrinkling capacities of skin," *Skin Research and Technology*, vol. 8, pp. 148-154, 2002.
- [35] K. Sauermann, S. Clemann, S. Jaspers, T. Gambichler, P. Altmeyer, K. Hoffmann, and J. Ennen, "Age related changes of human skin investigated with histometric measurements by confocal laser scanning microscopy *in vivo*," *Skin Research and Technology*, vol. 8, pp. 52-56, 2002.
- [36] M. J. Koehler, S. Zimmermann, S. Springer, P. Elsner, K. König, and M. Kaatz, "Keratinocyte morphology of human skin evaluated by *in vivo* multiphoton laser tomography," *Skin Research and Technology*, vol. 17, pp. 479-486, 2011.
- [37] S. G. Lagarrigue, J. George, E. Questel, C. Lauze, N. Meyer, J. M. Lagarde, M. Simon, A. M. Schmitt, G. Serre, and C. Paul, "In vivo quantification of epidermis pigmentation and dermis papilla density with reflectance confocal microscopy: Variations with age and skin phototype," *Experimental Dermatology*, vol. 21, pp. 281-286, 2012.
- [38] R. A. Briggaman and C. E. Wheeler, Jr., "The epidermal-dermal junction," *Journal of Investigative Dermatology*, vol. 65, pp. 71-84, 1975.